Report 5, 1992

DISTRIBUTED PARAMETER MODELS FOR THE LAUGARNES GEOTHERMAL FIELD, SW-ICELAND AND THE CENTRAL DEPRESSION OF DANUBE BASIN, S-SLOVAKIA

Dr. Marián Fendek,
UNU Geothermal Training Programme,
Orkustofnun - National Energy Authority,
Grensasvegur 9,
108 Reykjavik,
ICELAND

Permanent address:
Dionýz Štúr Institute of Geology,
Mlynská dolina 1,
817 04 Bratislava,
CZECHO - SLOVAKIA

ABSTRACT

The report describes distributed parameter models of two geothermal reservoirs. The basic equations of the problem are derived and the reservoir behaviour of two different geothermal fields is analyzed.

The first field evaluated is the Laugarnes geothermal field in Reykjavik, SW-Iceland. In this case the calibration of the model was made on the basis of 30 years observation of the reservoir response to production. A good fit was achieved with the model for drawdown. For the calibration of the model, the measured monthly average production of 16 wells from 1961 to 1991 was used. The obtained reservoir parameters were used for the future prediction of the reservoir behaviour at different constant production rates until the year 2012. A constant decline of the water level and silica content is observed. Based on the trend of the curve for the measured and calculated drawdown obtained from the distributed groundwater flow model, it is quite obvious that with present production, no steady-state condition in the reservoir will be reached during the period.

The second field evaluated in this study is the central depression of the Danube basin in S-Slovakia. Because of insufficient number of measured data from existing wells, only the theoretical model of the field was tested. The coefficient of transmissivity was estimated from well tests and hydrodynamically controlled measurements. For this reservoir, measured data (i.e. discharge, water level and temperature) from previous years which are necessary to estimate the recharge or leakage coefficient are not available. However, at a certain five-year production period when geothermal water exploitation was mainly seasonal, measurements were done only once a year and from this scarce data, no decline in water level and temperature was observed. Results from the distributed parameter model show that after 10 years of producing 308 l/s of geothermal water, the reservoir has a relatively steady-state condition. When production is increased to 732 l/s, the future drawdown is predicted to increased to 20-50 m in the various parts of the central depression. The calculations also showed no cooling during the production period as well as for the future production period.

TABLE OF CONTENTS

LIST OF FIGURES

LIST OF TABLES

1. INTRODUCTION

The author had the opportunity to become acquainted with reservoir engineering methods during his six months training at the United Nations University Geothermal Training Programme at Orkustofnun (The National Energy Authority) in Reykjavík, Iceland in 1992. The course started with two months of lectures on various special subjects concerning all aspects of exploration, production and use of geothermal energy around the world. It was followed by an eight day field trip to the main high and low temperature fields of Iceland. The special subsequent course in reservoir engineering consisted of:

- attending special lectures on modelling and reservoir engineering;
- a review and study of advanced papers and publications on modelling;
- taking part in field well tests;
- the collection and evolution on the available data;
- practical work with different special programmes, created for a personal computer;
- writing a general report on modelling of the Laugarnes geothermal field in Iceland and the Central depression of the Danube basin in Slovakia.

In recent years, particularly during the last decade, the use of geothermal reservoir modelling has grown significantly. Modelling has turned out to be a very effective method for analyzing data from geothermal reservoirs, as well as for estimating a geothermal field's future behaviour and its production potential. Numerous quantitative models have been developed for different geothermal fields all over the world (Bodvarsson et al., 1986).

In a broad sense, geothermal reservoir models can be divided into two categories:

1. **Simple models** are in many cases adequate idealization of real situations (Grant et al., 1982). They have the great advantage of being simple, they do not require the use of large computers and they are inexpensive to use. But simple models can neither consider spatial variation in the properties and parameters of a reservoir nor its internal structure. According to their methods of calculation, simple models can be further divided into two subcategories:

    a. <u>Distributed analytical models</u> in which, for example, the pressure response is given by an analytical function;
    b. <u>Lumped parameter models</u> which use very few blocks to represent the geothermal system.

2. **Numerical models** are very general mathematical models that can be used to simulate geothermal reservoirs in as much detail as desired. If only a few grid blocks are used, one has the equivalent of a lumped parameter model, but several hundred or thousand grid blocks can be used to simulate entire geothermal systems. But detailed numerical modelling of a geothermal reservoir is time consuming, costly and requires large amounts of field data. Numerical models can be further divided into two subcategories:

    a. <u>Natural-state models</u> developed for studies of the natural (unexploited) behaviour of geothermal systems;
    b. <u>Exploitation models</u> developed for studies of geothermal reservoirs under exploitation (Bodvarsson et al., 1986).

In both cases, the models can only be as good as the data upon which they are based. Substantial monitoring programs are, therefore, essential.

The research study described in this report was carried out during the last two months of the special geothermal course. The author was carefully supervised by his advisers Dr. Snorri Pall Kjaran and Mr. Sigurdur Larus Holm throughout the specialized course period.

The main scope of the study was the calibration of reservoir parameter values and the prediction of the future response of the reservoirs due to different production rates. The calibration and prediction processes were performed by using the numerical AQUA programme package developed by Vatnaskil Consulting Engineers (1991).

The main purpose of the course was to provide the author with the necessary knowledge and experience for later use in his home country.

2. DISTRIBUTED PARAMETER MODEL

Aquifer models can be classified in several ways. We can distinguish between continuous models, and those with a discrete distribution of parameters. The simplest type of a geothermal reservoir model is the lumped parameter model. In this case only the lumped mass within the system and what crosses the boundaries is taken into account. In this model, time is the only independent variable, and the system can, therefore, be described mathematically by the use of ordinary differential equations and, as a result, analytical solutions for the average reservoir parameter can be obtained. Models with distributed parameters, i.e., where the properties of fluid and rock can vary in space, demand larger computers. Models with distributed parameters are often too complex to be treated analytically. In these cases a numerical approach is used (Bodvarsson and Witherspoon, 1989).

At present, with high-speed computers widely available, numerical models are being used extensively for geothermal reservoirs. We can consider, in principle, two types of models: **finite difference models** and **finite elements models**. The concept of elements (the subareas delineated by the lines connecting nodal points) is fundamental to the development of equations in the finite element method. Mainly triangular elements are used, but quadrilateral or other elements are also possible. In the difference method, nodes may be located inside cells, or at the intersection of grid lines. The object of modelling is to predict the values of unknown variables (for example groundwater head or concentration of a contaminant) at nodal points. Models are often used to predict the effect of pumping on groundwater levels. However, before a predictive simulation can be made, the model should be calibrated and verified. The process of calibration and verification of the model is the content of the following chapters of this report.

2.1 Theoretical basis with emphasis on the AQUA programme package

AQUA is a programme package developed by Vatnaskil Consulting Engineers (1991) to solve the groundwater flow and transport equations using the Galerkin finite element method. The basis for the mathematical model is the following differential equation:

$$a\frac{\partial u}{\partial t} + b_i\frac{\partial u}{\partial x_i} + \frac{\partial}{\partial x_i}\left(e_{ij}\frac{\partial u}{\partial x_j}\right) + fu + g = 0 \tag{1}$$

The model is two dimensional, and indices **i** and **j** indicate the **x** and **y** coordinate axes.

AQUA can be used on IBM PC/XT/AT or compatible computers and requires 4 MB memory RAM, EGA graphics card and display, hard disk, maths coprocessor and optional hardware: digitizer, mouse, graphical printer, HP-plotter or compatible. The program package requires about 4.2 MB of disk space. As a guideline for an example which has less than 5,000 nodes, total memory requirement (memory and disk space) is 9-10 MB, and for a 10,000 nodes example, one needs 40-45 MB for total free memory.

2.1.1 Flow model

For transient groundwater flow, Equation 1 reduces to

$$a\frac{\partial u}{\partial t} + \frac{\partial}{\partial x_i}\left(e_{ij}\frac{\partial u}{\partial x_j}\right) + fu + g = 0 \tag{2}$$

For a confined groundwater flow in a leaky aquifer, the parameters in Equation 2 are defined as

$$u = h;\ e_{ij} = T_{ij};\ f = 0;\ g = Q + (k/m)/(h_0\text{-}h);\ a = -S$$

By using **x** and **y** instead of the indices Equation 2 then reads

$$\frac{\partial}{\partial x}\left(T_{xx}\frac{\partial h}{\partial x}\right) + \frac{\partial}{\partial y}\left(T_{yy}\frac{\partial h}{\partial y}\right) + \frac{k}{m}(h_o - h) + Q = S\frac{\partial h}{\partial t} \tag{3}$$

where

h	*- groundwater head [m];*
T_{xx}	*- transmissivity along principal axis [m^2/s];*
T_{yy}	*- transmissivity perpendicular to the principal axis [m^2/s];*
Q	*- pumping/injection rate [m^3/s];*
k/m	*- leakage coefficient, where k is the permeability of the semipermeable layer; and m its thickness [1/s];*
S	*- storage coefficient.*

For long term exploitation, storage in the reservoir is controlled by compressibility of the water and the rock in terms of the elastic storage coefficient as in confined aquifers and by the delayed yield effect. In this case, the equation for the transient groundwater flow is:

$$\frac{\partial}{\partial x}\left(T_{xx}\frac{\partial h}{\partial x}\right) + \frac{\partial}{\partial y}\left(T_{yy}\frac{\partial h}{\partial y}\right) + \frac{k}{m}(h_o - h) + Q = S\frac{\partial h}{\partial t} + \alpha\phi\int_0^t \frac{\partial h}{\partial t}e^{-\alpha(t-\tau)}\,d\tau \tag{4}$$

where

ϕ	*- effective porosity;*
α	*= $1/\kappa$, and κ is a time constant [s].*

To obtain an expression for the numerical solution of Equation 4 the following way is used:
Step *n*

$$i_n = \alpha n\int_0^{t_n} \frac{\partial h}{\partial t}e^{-\alpha(t-\tau)}\,d\tau \tag{5}$$

and step $n + 1$

$$i_{n+1} = \alpha n\int_0^{t_{n+1}} \frac{\partial h}{\partial t}e^{-\alpha(t_{n+1}-\tau)}\,d\tau \tag{6}$$

The integral can be rewritten as

$$i_{n+1} = e^{-\alpha\Delta t}i_n + \alpha n e^{-\alpha(t_n+\Delta t)}\left[\frac{1}{\alpha}e^{\alpha\tau}\right]_{t_n}^{t_{n+1}}\frac{(h_{n+1}-h_n)}{\Delta t} \tag{7}$$

Finally

$$i_{n+1} = e^{-\alpha\Delta t} i_n + \frac{n}{\Delta t}(h_{n+1} - h_n)(1 - e^{-\alpha\Delta t}) \tag{8}$$

Now Equation 4 can be approximated by the following numerical expression:

$$-K[\theta h_{n+1} + (1-\theta)h_n] = \frac{1}{\Delta t} M(h_{n+1} - h_n) + L[\theta i_{n+1} + (1-\theta)i_n] \tag{9}$$

where θ is equal to 1, as the classic implicit approximation.

For steady state, Equation 1 reduces to

$$\frac{\partial}{\partial x_i}\left(e_{ij}\frac{\partial u}{\partial x_j}\right) + fu + g = 0 \tag{10}$$

where we define

$u = h$; $e_{ij} = T_{ij}$; $f = 0$; $g = Q + \gamma$ and
$\gamma = R$ (infiltration rate) for an unconfined horizontal aquifer [mm/year], or
$\gamma = (k/m)(h_o - h)$ for a confined horizontal aquifer [m/s].

By using **x** and **y** instead of the indices, Equation 10 then reads

$$\frac{\partial}{\partial x}\left(T_{xx}\frac{\partial h}{\partial x}\right) + \frac{\partial}{\partial y}\left(T_{yy}\frac{\partial h}{\partial y}\right) + Q + \gamma = 0 \tag{11}$$

In the AQUA model, the following boundary conditions are allowed

- **Dirichlet boundary condition**, the groundwater level, the piezometric head or the potential function is prescribed at the boundary;
- **Von Neumann boundary condition**, the flow at the boundary is prescribed by defining source nodes at the no-flow boundary nodes;
- **Cauchy boundary condition**, the boundary flow rate is related to both the normal derivative and the head.

2.1.2 Mass transport model

The AQUA program can solve the transient transport of mass in which case the parameters of Equation 1 are defined as follows:

$u = c$; $a = \phi b R_d$; $b_i = v_i b$; $e_{ij} = -\phi b D_{ij}$; $f = \phi b R_d \lambda + \gamma + Q$; $g = -\gamma c_0 - Q c_w$.

By using **x** and **y** instead of the indices, Equation 1 then reads

$$\frac{\partial}{\partial x}\left(\phi b D_{xx}\frac{\partial c}{\partial x}\right) + \frac{\partial}{\partial y}\left(\phi b D_{yy}\frac{\partial c}{\partial y}\right) - v_x b\frac{\partial c}{\partial x} - v_y b\frac{\partial c}{\partial y} = \phi b R_d\frac{\partial c}{\partial t} + \phi b R_d \lambda c - (c_o - c)\gamma - Q(c_w - c) \tag{12}$$

The above equation applies to a local coordinate system within each element having the main axis along the flow direction. The dispersion coefficients are defined by

$$\phi D_{xx} = a_L v^n + D_m \phi \tag{13}$$

$$\phi D_{yy} = a_T v^n + D_m \phi \tag{14}$$

The retardation coefficient R_d is given by

$$R_d = 1 + \beta_c \frac{(1-\phi)\varrho_s}{\phi \varrho_l} \tag{15}$$

$$\beta_c = K_d \varrho_l \tag{16}$$

where

c	- *solute concentration [kg/m³];*
c_o	- *solute concentration of vertical inflow [kg/m³];*
c_w	- *solute concentration of injected water [kg/m³];*
v_x, v_y	- *velocity vector taken from the solution of the flow problem [m/s];*
a_L	- *longitudinal dispersivity [m];*
a_T	- *transversal dispersivity [m];*
v	- *velocity [m/s];*
D_m	- *molecular diffusivity [m²/s];*
ϕ	- *effective porosity;*
Q	- *pumping rate [m³/s];*
b	- *aquifer thickness [m];*
λ	- *exponential decay constant [1/s];*
K_d	- *distribution coefficient;*
ϱ_l	- *density of the liquid [kg/m³];*
ϱ_s	- *density of the porous medium [kg/m³];*
γ	- *R (infiltration rate) for unconfined horizontal aquifer [mm/year];*
γ	- *(k/m)(h_0 - h) for confined horizontal aquifer [m/s];*
β_c	- *retardation constant.*

2.1.3 Heat transport model

For the heat transport model, the parameters in Equation 1 are defined as follows:

$$u = T;\ a = \phi b R_h;\ b_i = v_i b;\ e_{ij} = -bK_{ij};\ f = \gamma + Q;\ g = -\gamma T_o - Q T_w$$

By using **x** and **y** instead of the indices, Equation 1 then reads

$$\frac{\partial}{\partial x}\left(bK_{xx}\frac{\partial T}{\partial x}\right) + \frac{\partial}{\partial y}\left(bK_{yy}\frac{\partial T}{\partial y}\right) - v_x b\frac{\partial T}{\partial x} - v_y b\frac{\partial T}{\partial y} = \phi b R_h \frac{\partial T}{\partial t} - (T_o - T)\gamma - (T_w - T)Q \tag{17}$$

The above equation also applies to a local coordinate system within each element having the main axis along the flow direction.

The heat dispersion coefficients are given by

$$K_{xx} = a_L v^n + D_h \phi \tag{18}$$

$$K_{yy} = a_T v^n + D_h \phi \tag{19}$$

The heat retardation coefficient R_h is given by

$$R_h = 1 + \beta_h \frac{(1-\phi)\varrho_s}{\phi \varrho_l} \tag{20}$$

$$\beta_h = \frac{C_s}{C_l} \tag{21}$$

where

T	- *temperature [°C];*
T_o	- *temperature of the vertical inflow [°C];*
C_l	- *specific heat capacity of the liquid [kJ/kg °C];*
C_s	- *specific heat capacity of the porous medium [kJ/kg °C];*
β_h	- *retardation constant;*
D_h	- *heat diffusivity [m^2/s].*

The other parameters are defined as previously.

For both the transport models, two kinds of boundary conditions are allowed:

- **Dirichlet boundary conditions**, the concentration or temperature is specified at the boundary.
- **Von Neumann boundary condition**, the concentration gradient or the temperature gradient is set to zero indicating convective transport of mass or heat through the boundary.

3. THE LAUGARNES GEOTHERMAL FIELD, SW-ICELAND

Exploitation of hot ground water by wells in the Laugarnes field increased rapidly from 1958. Then about 30 l/s flowed freely from a few shallow wells until 1969, when a maximum of 330 l/s was pumped from 11 supply wells with depths up to 2,198 m.

An investigation on the response of the piezometric surface in the area to increased pumping was begun in 1965 and continued through 1969. The investigation was conducted by automatic water stage recorders and by periodic measurements of water levels in non-pumping observation wells. It was initiated by the Department of Natural Heat of the National Energy Authority of Iceland in close cooperation with the Reykjavik Municipal District Heating Service.

The optimal production strategy of a geothermal field cannot be obtained without using a good performing reservoir model. It should give a clear picture about all physical, chemical and reservoir parameters, and the obtained results should be comparable to those of field measurements. The past, present and future exploitation of the geothermal field must be in compliance with the created model. All plans for changing the production rate from the reservoir should be carefully checked with it. The drilling of new boreholes, their situation and casing design, possible reinjection options for recovering the water level, changes of the chemcial concentration and heat losses due to interaction with another aquifer should be taken into consideration, only after addressing the reservoir model. As a final result, it should reward its users with the best economical solution for their needs.

3.1 The main features of the Laugarnes geothermal field

3.1.1 Locality

The Laugarnes low-temperature field is located inside Reykjavik, in the southwestern part of Iceland (Figure 1). The elevation of the area ranges from 15 to 40 m above sea level. It is one of the three major geothermal areas within a radius of 6 kilometers from the center of Reykjavik. The others are the Ellidaar and Seltjarnarnes fields (Figure 1).

3.1.2 Hydrogeology

The Reykjavik area lies 8-10 km north of the volcanically active Reykjanes rift zone. It is located in Plio-Pleistocene volcanics on the southern outskirts of the Kjalarnes central volcano (Fridleifsson, 1973).

The Reykjavik area is covered by horizontal olivine tholeiite basalts of late interglacial age, down to a depth of

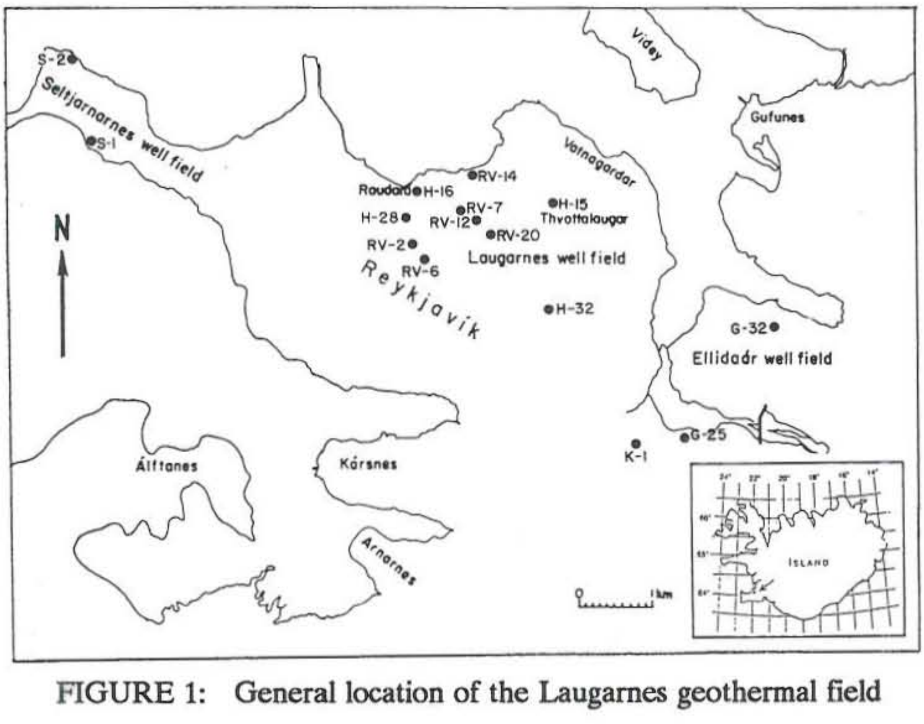

FIGURE 1: General location of the Laugarnes geothermal field

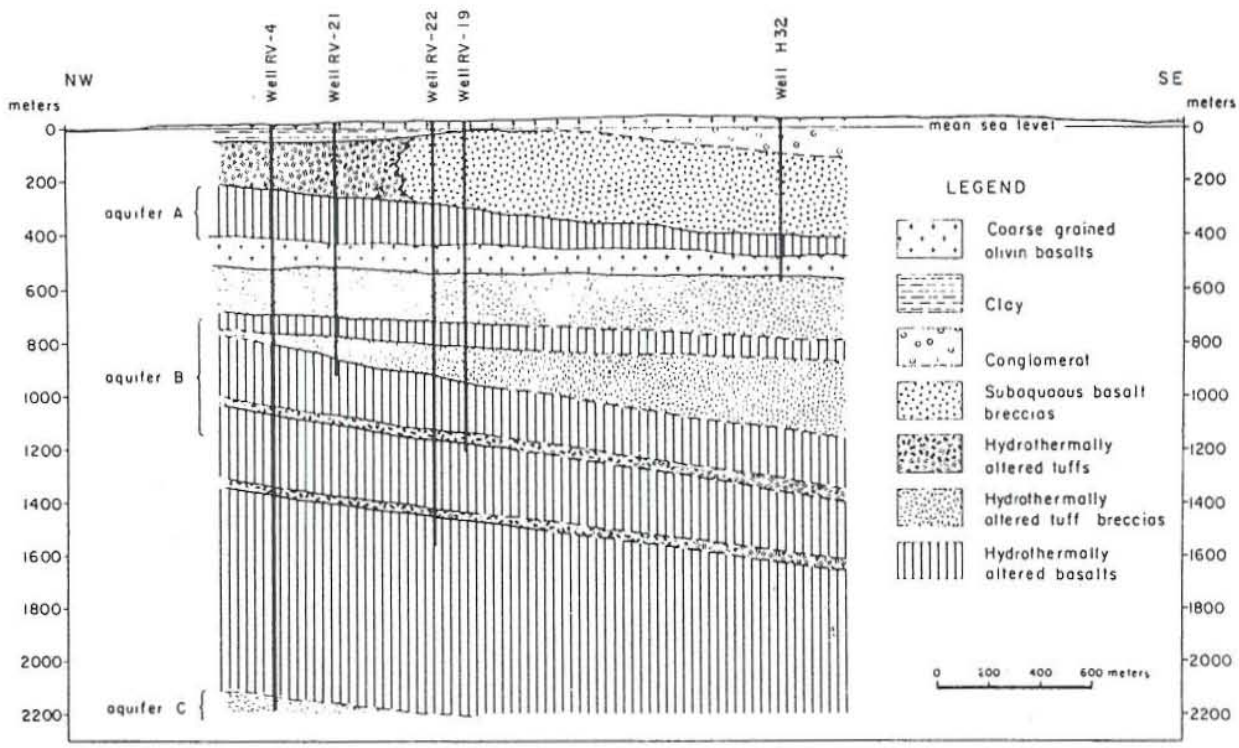

FIGURE 2: Generalized NW-SE geologic cross-section through the Laugarnes area

30-50 m (Thorsteinsson and Eliasson, 1970). Underneath this lava flow there are found mostly marine sediments of up to 60 m in thickness, which are layered on a major discordance. Beneath, alternating lavas and hyaloclastites are found. This sequence is of Plio-Pleistocene age. Thick hyaloclastite formations are common in the upper 500-1,000 m, but basaltic lavas are predominant in the lower parts of the wells, which are commonly up to 2 km deep.

The Plio-Pleistocene strata in the Laugarnessvæði area appears to dip 3-12 degrees to the southeast (Thorsteinsson and Eliasson, 1970). This strata occurs at 250-300 m lower elevation in wells of the Ellidaar area.

Aquifers are predominantly found at the contacts of lavas and hyaloclastites. The Laugarnes geothermal area has been found to be fed by three aquifers (Thorsteinsson and Eliasson, 1970). **Aquifer A** with water of 110-120°C extends from 250-650 m, **aquifer B** with water of 135°C from 730-1,250 m and **aquifer C** with water temperature of 146°C, below 2,150 m. Tuffs and sediments act as aquicludes between the aquifers while scoriaceous and fractured contacts between individual lava flows are permeable. Because each lava flow is a lens between overlying and underlying flows, the permeable zones within each aquifer are not continuous but may merge with those of adjacent flows. A geological and hydrogeological cross-section is shown in Figure 2. Aquifer B is the main aquifer with a contribution of 80%. Mixing of these waters yields an average **well discharge temperature of 125-130°C.**

The recharge area of the Laugarnes area has been mapped by deuterium (Arnason, 1977). By comparing the deuterium content of the precipitation in Iceland to that of the geothermal water, the Langjökull area has been shown to provide the recharge for the Laugarnessvæði geothermal field.

As in the Laugarnes area, aquifers in the Ellidaar area occur at contacts between hyaloclastites and lavas. The Ellidaar area is fed by at least two different groundwater systems. The northern part of the Ellidaar area is probably fed by the same recharge area as the Laugarnes area. The other recharge area for the southern part of this geothermal field is most likely east of Reykjavik, at a distance of less than 45 km (Arnason and Tomasson, 1970; Tomasson et al., 1975).

Tomasson et al. (1975) described results from measured surface thermal gradients in shallow drillholes in Reykjavik. The high surface thermal gradients inside the thermal areas are due to localized transport of water from the thermal systems at depth to the surface. This is best demonstrated in the Laugarnes area, where the highest surface gradients are measured (400°C/km). Prior to exploitation about 10 l/s of 88°C water issued in free flow from thermal springs in that area, whereas, only minor natural thermal activity was found in the other areas in Reykjavik. There is very little or no transport of water from depths in the rocks between the thermal areas, and the depths of the gradient drill holes (at least down to several hundred meters) has little influence on the measured gradient outside the thermal areas. The surface gradient of 0°C/km to the southeast of the thermal areas is due to cold groundwater penetrating young volcanic rocks. This cold groundwater zone has been found to reach down to 750 m (measured in a hole 986 m deep) in the volcanic zone 11 km south of the Ellidaar area (Palmasson, 1967).

Outside the thermal fields the thermal gradient is about 100°C/km. The reverse temperature gradients found in the Ellidaar and Reykir fields can only be accounted for by the circulation of cold water at depth. This cooling effect might be similar to the surface cooling effect observed southeast of Reykjavik.

3.1.3 Production history and utilization

The exploitation of geothermal water in the Laugarnes area began in 1928-1930 by the drilling of 14 small diameter wells near the Thvottalaugar hot spring. The depth of the deepest well was 246 m; collectively, the wells yielded 15-20 l/s at a temperature of 95°C, as compared to 5-10 l/s previously issuing from the spring.

Drilling was resumed, first in 1940 by the drilling of two wells, 650 and 760 m in depth at Thvottalaugar and at Raudará, and again in 1956-1959 by the drilling of 16 wells, 260-696 m deep, 1-2 km west of the Thvottalaugar wells. The aggregate flow from these wells in 1959 was about 60 l/s, 90-98°C. During the drilling phase of 1959-1963, 22 wells were drilled by the rotary method to depths of 650-2,198 m. The individual well flow rates ranged from 1 l/s to more than 50 l/s. Five additional deep wells have since been drilled, in 1968 and 1969, and 1978-1982, to depths of 1,359-3,085 m one of them, RV-34, being the deepest well in Iceland. In the last decades, 11 wells, 1,025-1,647 m in depth, have also been drilled in the Ellidaar area, few wells in the Seltjarnarnes area and one well in Kopavogur near the Ellidaar well field.

The wells are of the open hole type. Casing is cemented in place to a depth required to prevent collapse of unconsolidated shallow formations and exclude surface waters and the hole left open below the casing point. Well data of supply wells and principal observation wells are given in Table 1 and the location of wells is shown in Figure 3.

Up to the year 1960, when deep-well turbine pumps were first installed, withdrawal of water from the wells was by flow on the head. Since 1967, however, it has been exclusively through deep-well turbine pumps from 11 supply wells. Prior to 1962, flow rates were estimated from periodic flow measurements but have since then been metered.

Withdrawal rates were relatively uniform during the period 1957-1962, when withdrawal was predominantly by flow on the head but those subsequent to 1962 vary according to seasonal demand, being about three times as heavy in the winter season, October until March, than in the

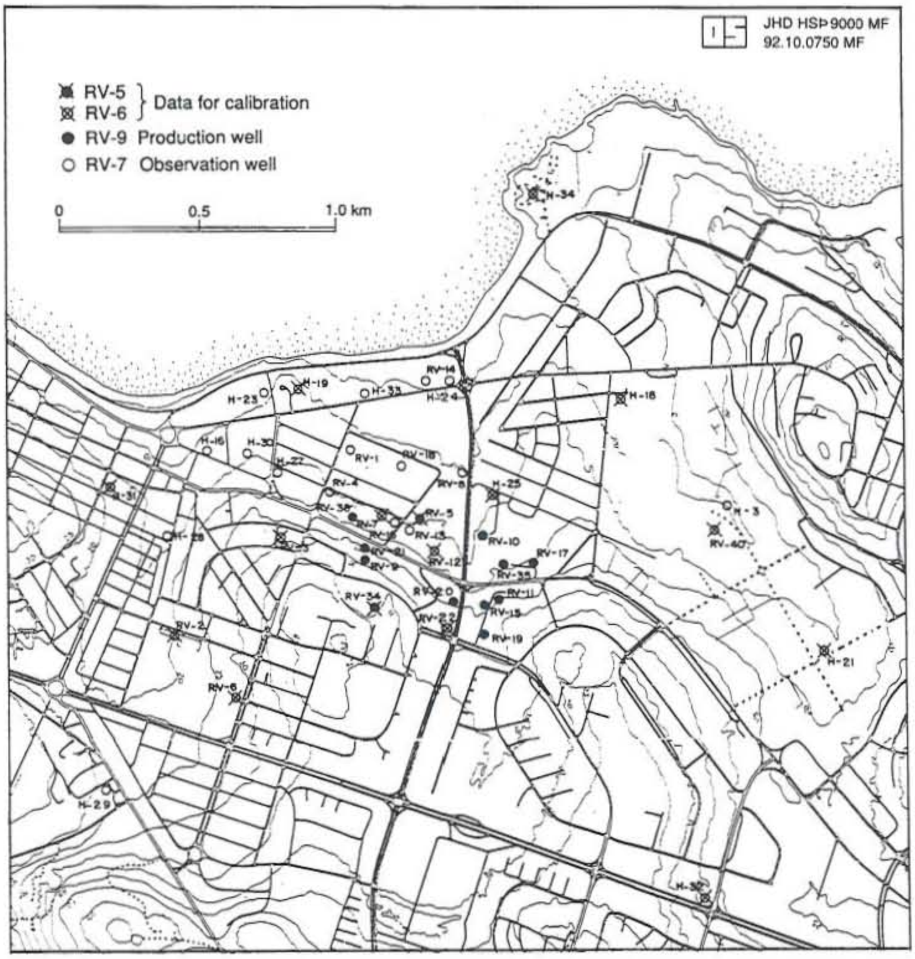

FIGURE 3: Location of wells in the Laugarnes field

warmer season, April until September.

The Laugarnes area has been exploited by the Municipal District Heating Service of Reykjavik (Hitaveita Reykjavikur) since 1928. Up to the present, more than 50 deep water wells have been drilled in the area producing hot water up to 130°C. The wells are not all connected to the water supply system due to reasons such as; they are too shallow, the water temperature is too low or the water yield of the wells is too small. Besides, some of the production wells have been taken off-line as an increasing amount of dissolved salts (sea water) in the geothermal water has caused depositions in downhole pumps. The yearly average production from this area since 1962 is shown in Figure 4.

3.2 Results from the calibration

The total surface area covered by the mesh is about 67.95 km^2. The model was created with 1,356 nodes and 2,627 elements. Thus, the boundaries are taken far enough away to avoid their influence on the solution. Boundary conditions for the distributed groundwater flow model are established based on resistivity and water level measurements. The no-flow boundary was established around the whole Laugarnes area and only a small part in the southeast area was used as boundary with constant potential. The boundary conditions which were used for the distributed model is shown in Figure 5.

TABLE 1: Well data in the Laugarnes area

Well no.	Year completed	Elevation [m a.s.l.]	Depth of well [m]	Depth of casing [m]	Temperature of water [°C]
RV-01	1962	12.04	1067	70	-
RV-02	1958	20.86	650	30	-
RV-03	1958	27.03	732	71	-
RV-04	1959	15.48	2198	69	135
RV-05	1959	15.07	741	68	130
RV-06	1959	27.63	765	99	-
RV-07	1959	16.90	752	94	-
RV-08	1960	11.01	1397	91	-
RV-09	1959	27.06	862	90	128
RV-10	1959	15.87	1306	92	130
RV-11	1962	25.72	928	112	130
RV-12	1962	17.74	1105	94	-
RV-13	1962	17.10	975	100	-
RV-14	1962	4.28	1026	101	-
RV-15	1962	24.72	1014	112	126
RV-16	1962	16.78	1300	256	-
RV-17	1963	21.59	634	93	122
RV-19	1963	28.09	1239	79	128
RV-20	1963	26.11	764	87	129
RV-21	1963	24.74	978	112	129
RV-22	1963	30.36	1583	83	-
RV-25	1968	29.50	1647	79	-
RV-32	1969	42.00	1359	100	-
RV-34	1978	33.00	3085	328	123
RV-35	1979	17.00	2857	276	119
RV-38	1982	16.50	1488	325	128
H-16	1943	12.36	770	17	-
H-18	1956	8.42	697	19	-
H-19	1956	10.20	471	-	-
H-27	1959	14.98	403	31	109
H-29	1959	19.82	249	33	-
H-32	1961	33.27	606	32	-
H-34	1961	7.00	399	-	-

As for the initial state, prior to production it was assumed that the reservoir water head was constant.

The production rates are taken as a monthly average for each supply well from 1962-1991. The initial values for transmissivity and storage coefficient are taken from the results of well tests. A number of tests have been made in wells in the Laugarnes area in order to determine values of the aquifer constants, transmissivity and storativity, and to locate impervious boundaries believed to exist between the three hydrothermal systems. The tests were conducted by observations of water levels in observation wells after a supply well was turned off or on, correction being made for previous trends in water levels. Because of variation in demand, the tests are of short duration, ususally less than 10-20 hours and are interfered with by operating supply wells, the discharge of which varies somewhat by variations in water level. Analysed by the THEIS

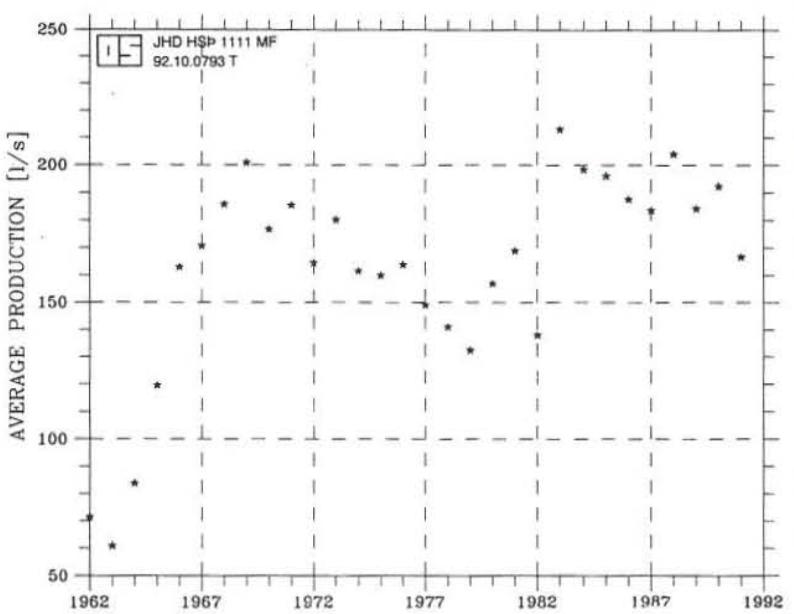

FIGURE 4: The yearly average production from the Laugarnes area

nonequilibrium method, the test data gave values ranging from 3.5 x 10^{-3} to 8.8 x 10^{-3} m^2/s for the **coefficient of transmissivity** and 3.9 x 10^{-5} to 3.2 x 10^{-4} for the **coefficient of storage** (Thorsteinsson and Eliasson, 1970).

The transmissivity, storage coefficient, anisotropy and porosity are determined by matching observed and calculated reservoir response. The **transmissivity** in the area covered by the model varies from 5.0 x 10^{-2} to 6.7 x 10^{-5} m^2/s. The low value for transmissivity is obtained along the northeast boundaries of

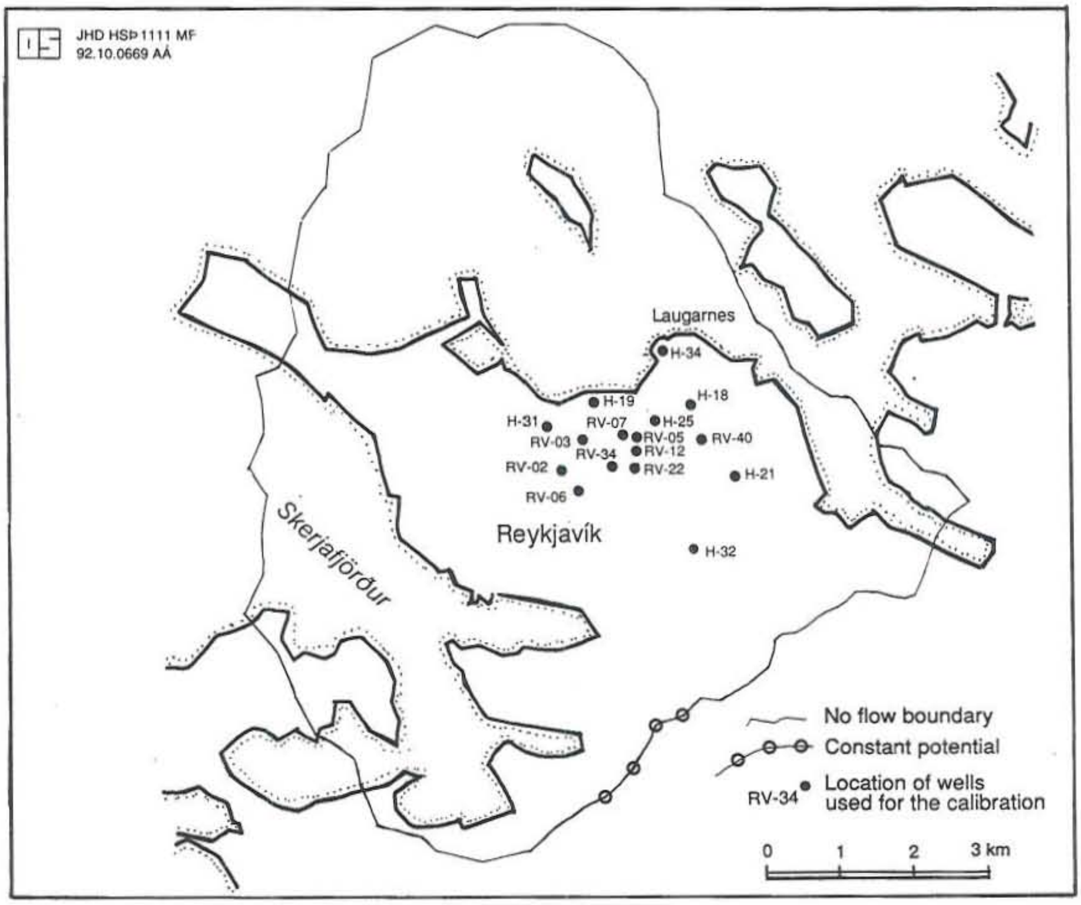

FIGURE 5: Boundary conditions of the model

Laugarnes area and the highest value is obtained in the center of this area (Figure 6).

The calibration started with the value of the **storage coefficient** in the range of 1.6 x 10^{-3} to 1.6 x 10^{-4} (Figure 7).

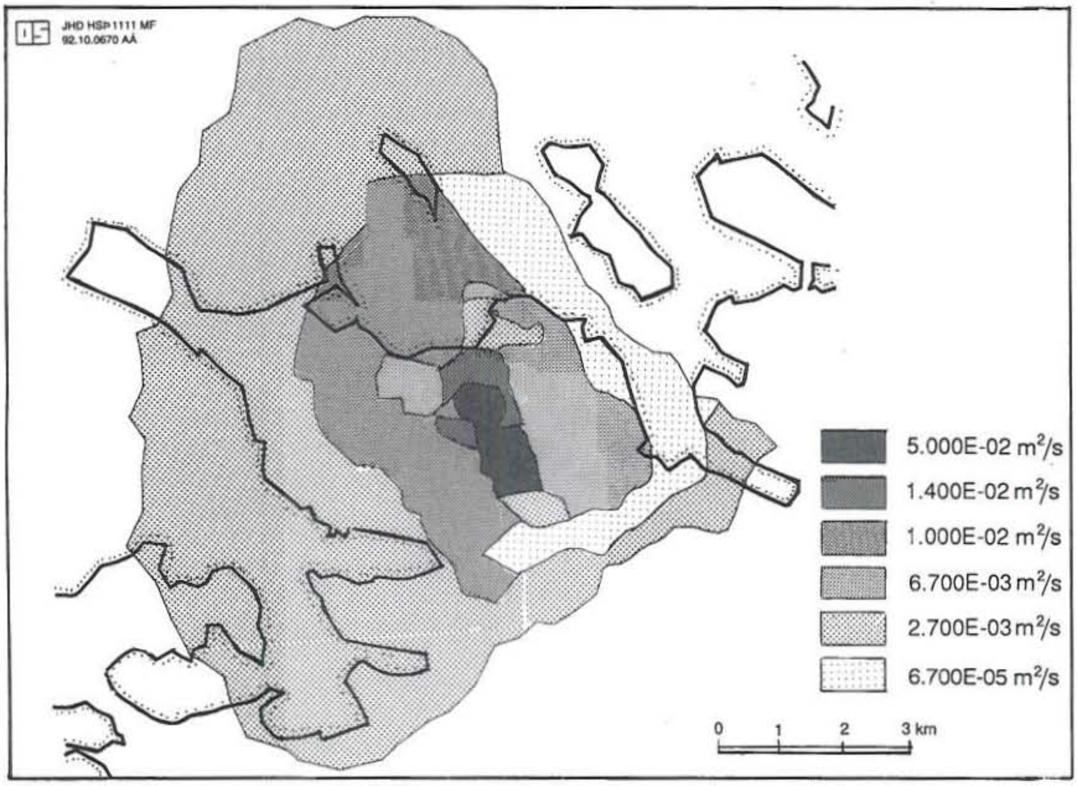

FIGURE 6: Map of transmissivity in the vicinity of wells

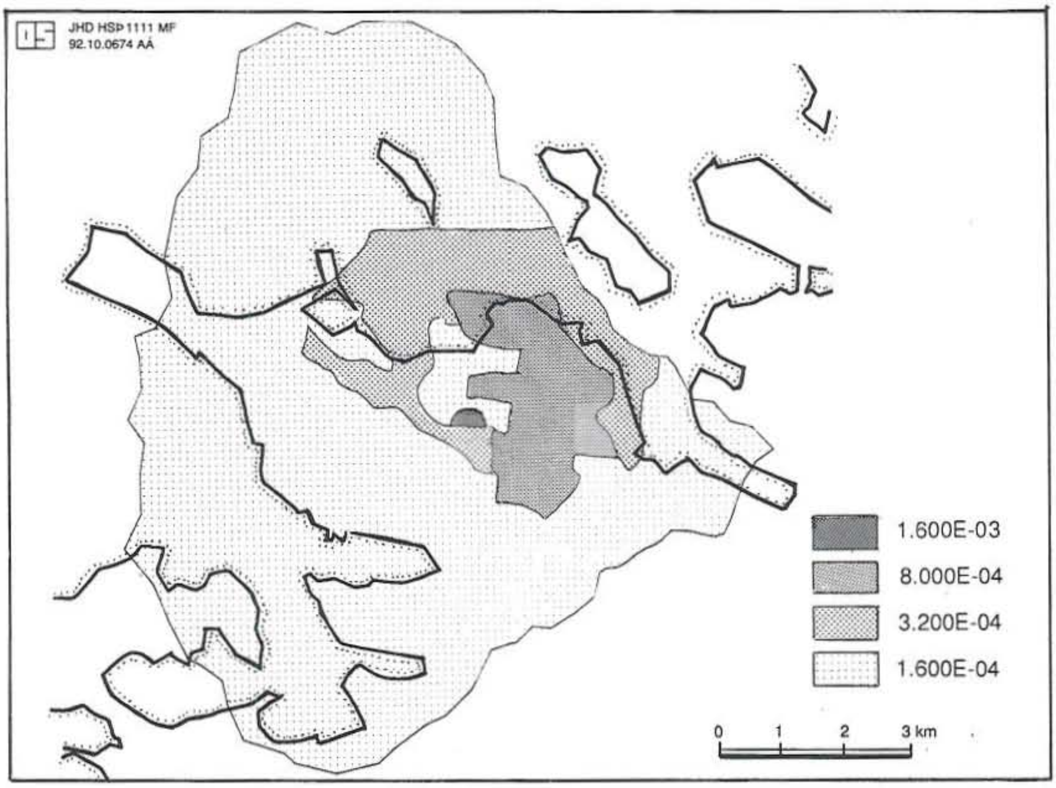

FIGURE 7: Map of storage coefficient

The long term effect of the exploitation was analysed, so the elastic storage coefficient and the delayed yield effect were taken into account. It was assumed that **porosity** of the reservoir is in the range of **0.0111-0.0108** and the **time constant 6,500 days** (Equation 4).

The **leakage coefficient** in the center area was taken to be in the range of **6×10^{-11} to 9×10^{-12}** s^{-1} and around the main production area the value of zero (0) was used (Figure 8) because almost no influence on temperature from the cold water recharge from above was observed.

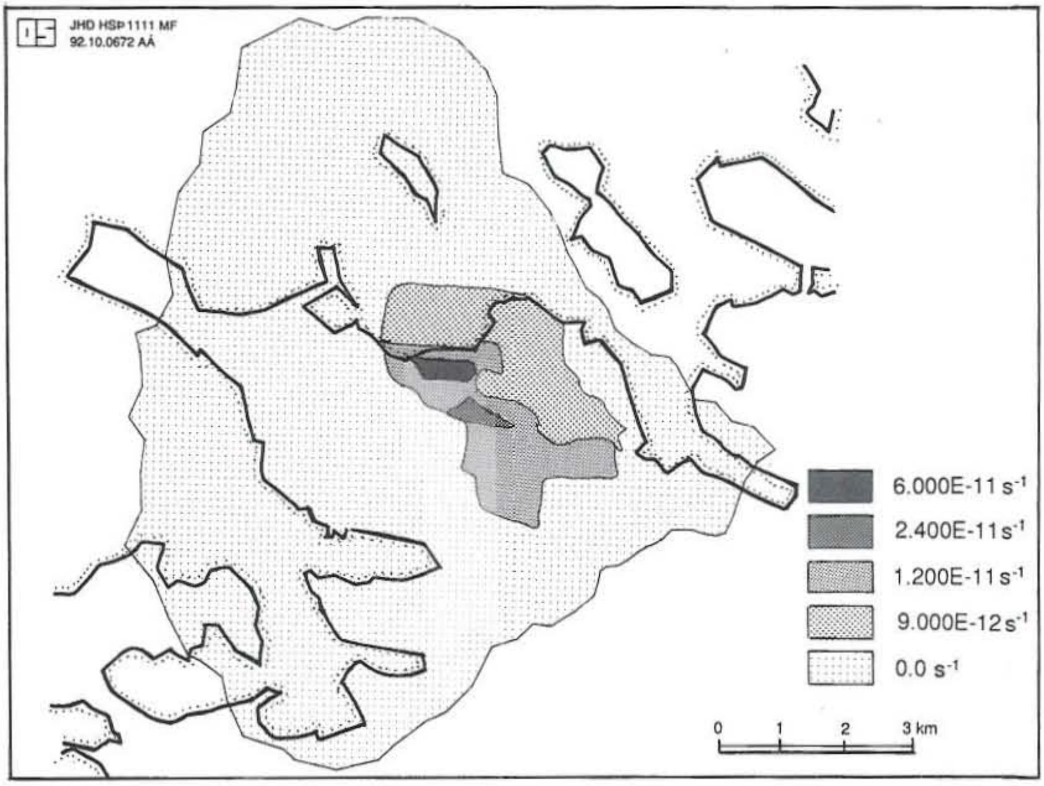

FIGURE 8: Areal distribution of leakage coefficient

Anisotropy is determined by anisotropy angle and by the ratio between transmissivity in **x** (T_{xx}) and **y** (T_{yy}) directions equal to is **0.0999. Anisotropy angles** range **from 50 degrees** in the western and southern part of Laugarnes area **to 120 degrees** in the center and northeast part of the area (Figure 9).

For the calibration of the model the measured data from 16 wells was used. The areal distribution of these wells is shown in Figures 3 and 5, and the results of the calibration are shown in Figures 10a, 10b, 10c and 10d. The best results were obtained for observation well RV-07. A good fit between measured and calculated drawdown values was obtained with the model for wells which are inside the main production area (RV-05, RV-34, RV-11, RV-22, H-25, H-19, RV-03, RV-06 and RV-02). A slightly worse fit between measured and calculated drawdown values was obtained with the model for wells which are around this production area (H-34, H-18, RV-40, H-21, H-32, H-31). The depth of these wells ranges from 249-770 m (refer to Table 1), they are relatively shallow and produce geothermal water from the top of the reservoir (refer to Figure 2, well H-32). This can be the reason why better results are not obtained with the two-dimensional AQUA model for these wells. The map of calculated drawdown is shown in Figures 11a and 11b.

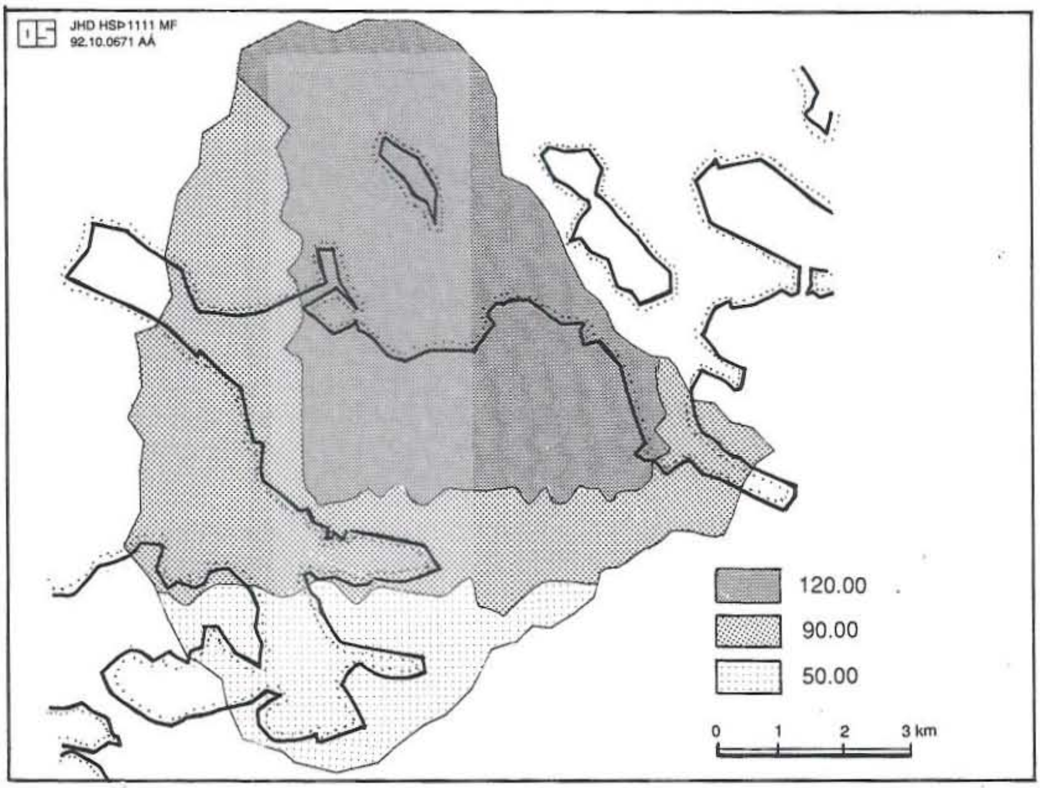

FIGURE 9: Areal distribution of anisotropy angle

Mass transport calculations can be used to estimate leakage coefficient and aquifer thickness. By fitting the calculated and measured values of silica concentration, the above-mentioned parameters can be calculated. Several measurements of silica concentration exist from each production well.

The silica content decreased due to the production (Hettling, 1984) and the induced leakage from above. The model parameters used for solving the mass transport of silica are as follows:

average initial concentration:	*160 mg/l*
average concentration in the top aquifer:	*22 mg/l*
a_T/a_L:	*0.16*
longitudinal dispersivity (a_L):	*80 m*
molecular diffusion:	$10^{-8}\ m^2/s$
aquifer thickness:	*800 m*

The concentration calculated with the model shows the same decreasing trend (Figure 12).

3.3 Future prediction of the reservoir response

After calibration, the model was used for the calculations of the drawdown until the end of year 2012. As a starting point for future prediction the reservoir state from 1992 is taken. The calculations were made with three different production rates which are shown in Table 2 for each supply well.

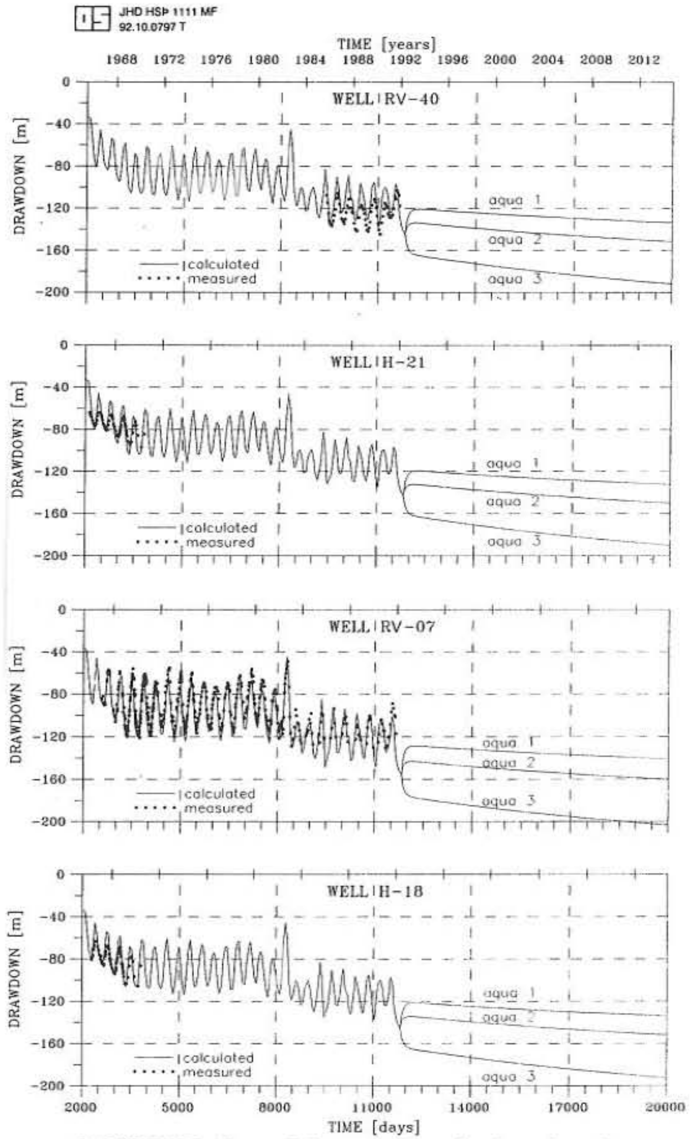

FIGURE 10a: Measured, calculated and prediction drawdown for wells RV-40, H-21, RV-07 and H-18

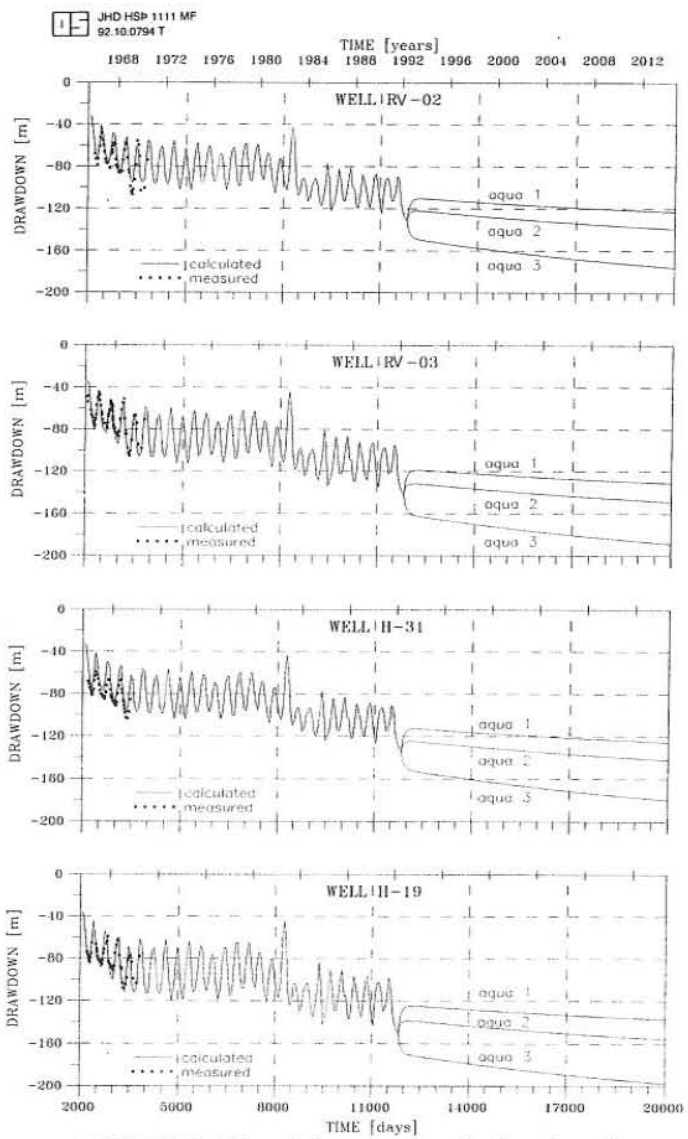

FIGURE 10b: Measured, calculated and prediction drawdown for wells RV-02, RV-03, H-31 and H-19

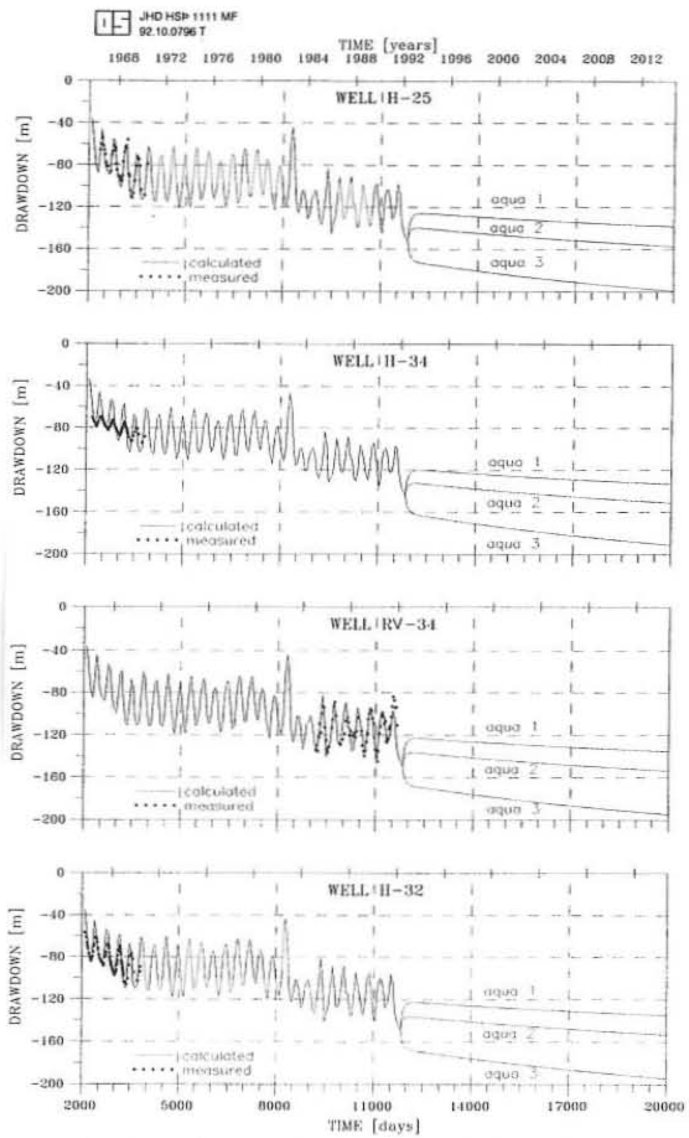

FIGURE 10c: Measured, calculated and prediction drawdown for wells H-25, H-34, RV-34 and H-32

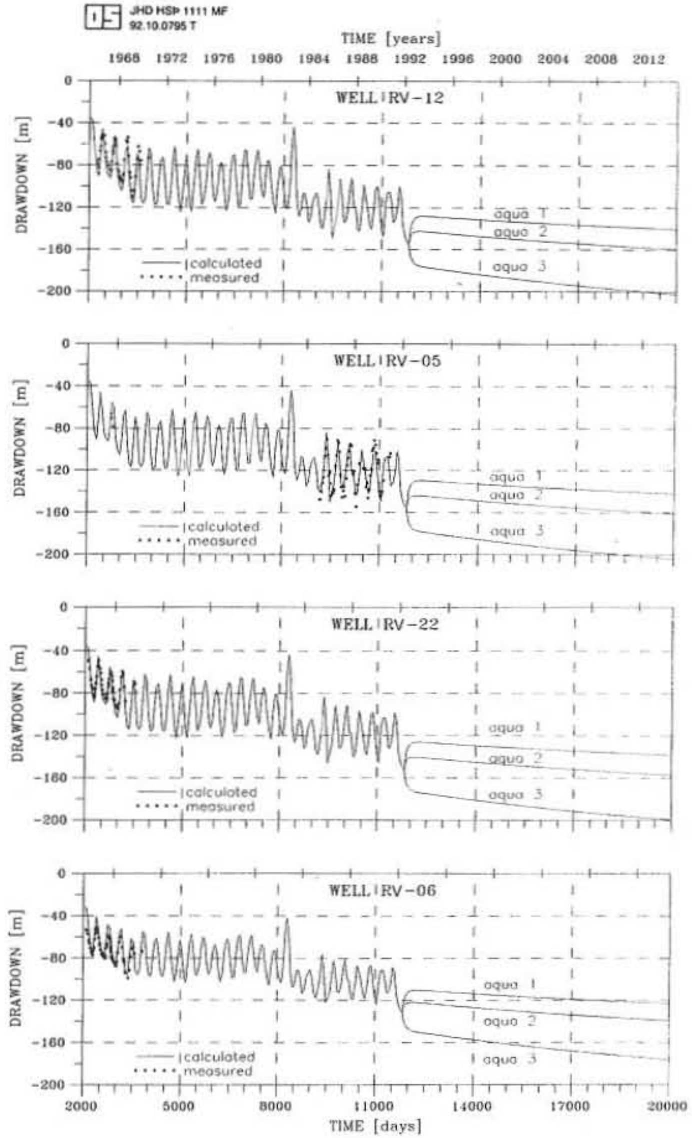

FIGURE 10d: Measured, calculated and prediction drawdown for wells RV-12, RV-05, RV-22 and RV-06

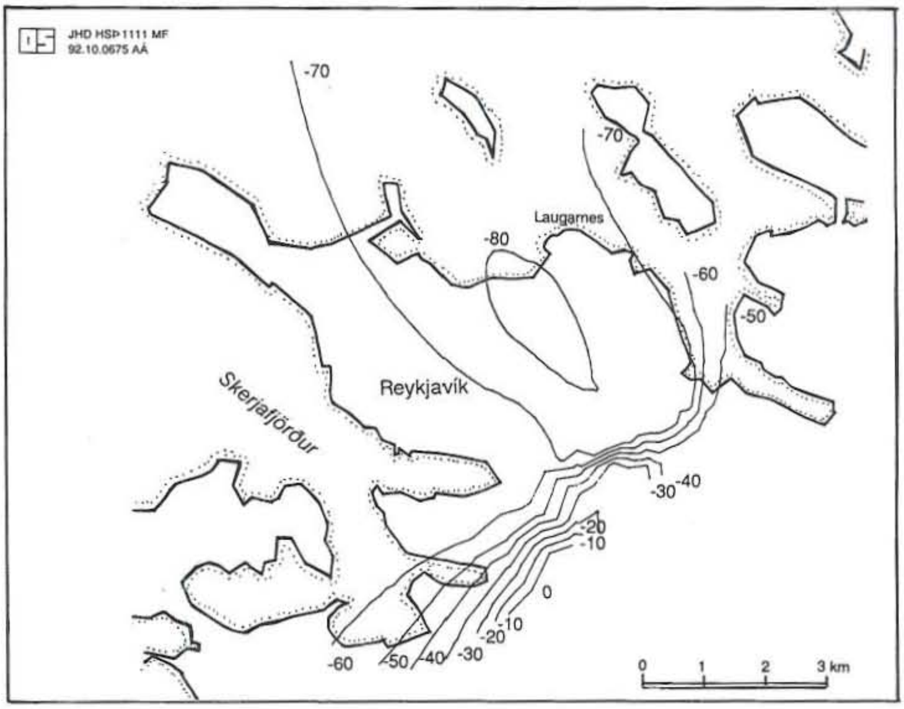

FIGURE 11a: Map of calculated drawdown [m], in 1982

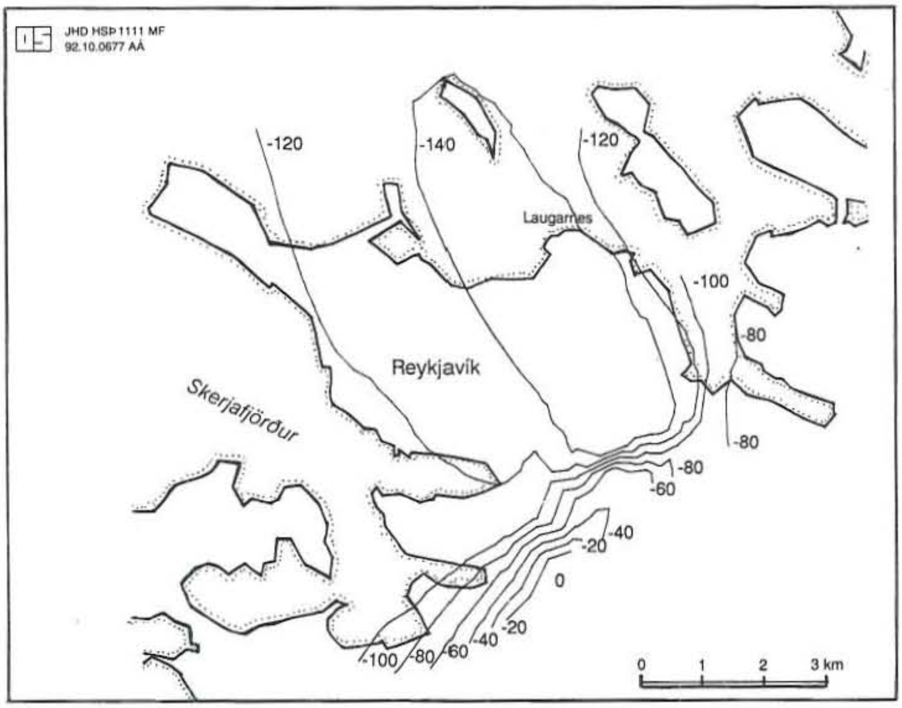

FIGURE 11b: Map of calculated drawdown [m], in 1991

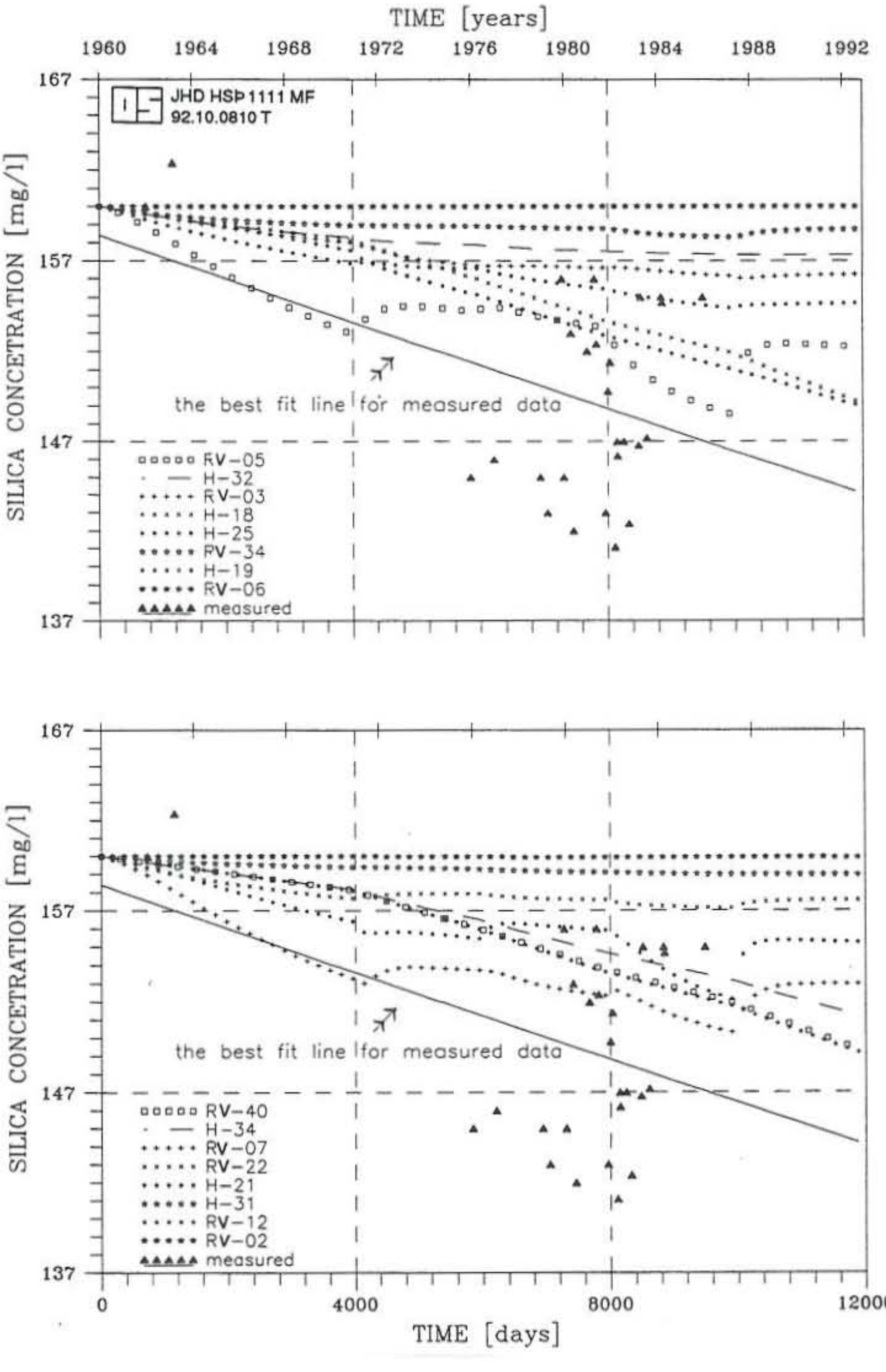

FIGURE 12: Silica contentration decline in the wells

TABLE 2: Future predictions for the yearly average production [l/s]

Well no.	Aqua 1	Aqua 2	Aqua 3
RV-05	53.0	53.0	65.0
RV-09	4.4	7.0	10.0
RV-10	12.5	15.0	20.0
RV-11	20.6	25.0	30.0
RV-15	13.2	16.0	20.0
RV-17	10.9	12.0	15.0
RV-19	21.2	25.0	30.0
RV-20	15.6	24.0	33.3
RV-21	30.8	30.0	45.0
RV-35	7.1	7.0	11.0
RV-38	10.0	20.0	30.2
Total:	199.3	234.0	309.5

The production rates under column aqua 1 represent the average production for last year (1991) which totals 199.4 l/s for all the wells. The values under column aqua 2 indicate that the average production is increased by 17.4% (total of 234 l/s) when compared to that of the actual values in the column under aqua 1. Furthermore, the values under column aqua 3 give the highest values for yearly average production rate and the total of 309.5 l/s is 55.5% higher than the values in aqua 1. The calculation results for the future predicions are shown in Figures 10a, 10b, 10c and 10d. All calculated curves of future drawdown show a lowering trend. The obtained **drawdown** is between **110-190 m** with a corresponding total yearly average production of **199.4-309.5 l/s** respectively. The results mentioned above are yearly average values and do not take into account the seasonal changes in production.

Future prediction for silica concentration shows the same decreasing trend as during the production period (Figure 13).

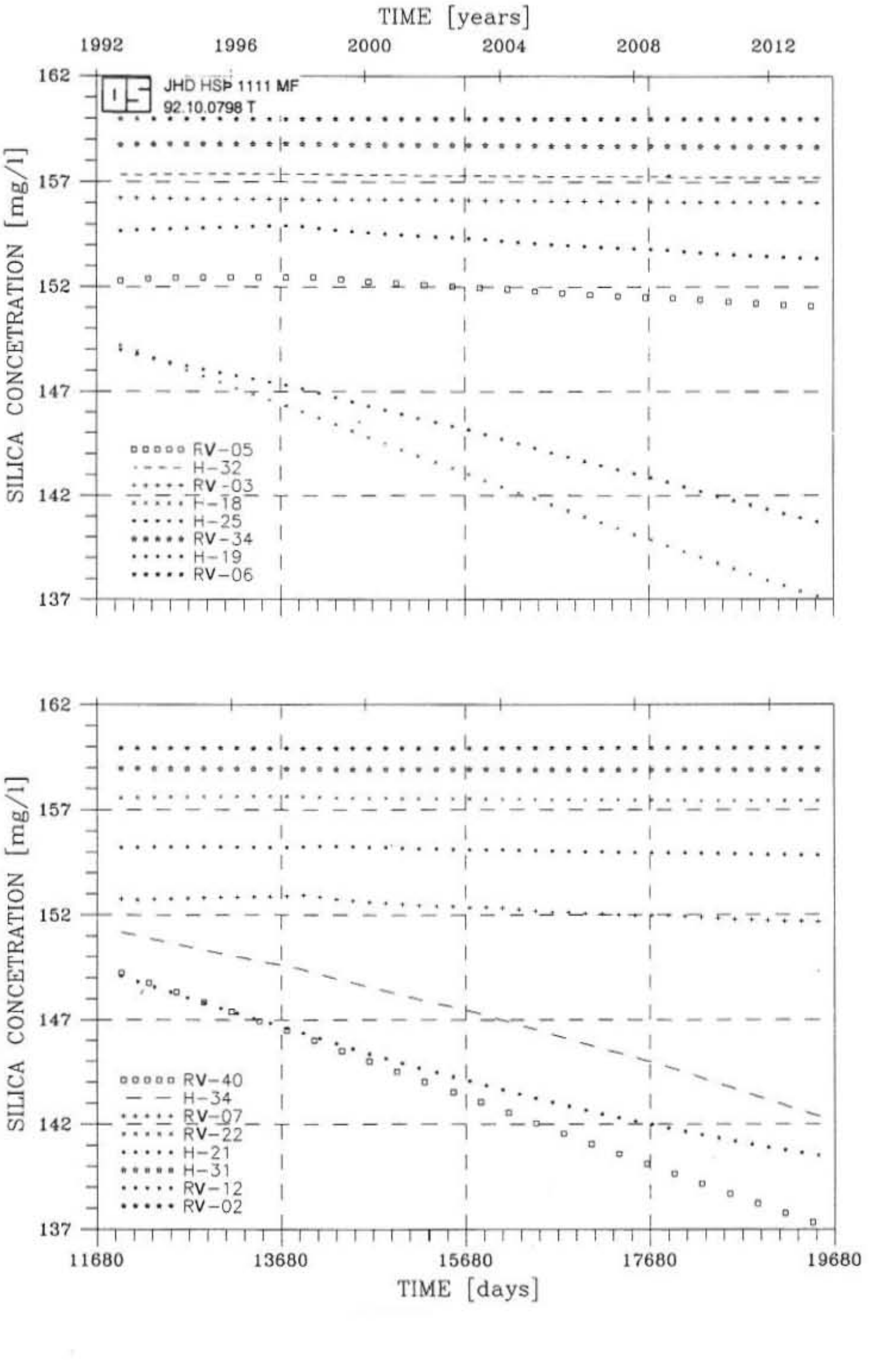

FIGURE 13: Future prediction of the silica concentration

4. THE CENTRAL DEPRESSION OF THE DANUBE BASIN, S-SLOVAKIA

4.1 The main features of the central depression of the Danube basin

The geothermal energy resources in Czecho-Slovakia are represented first of all by low temperature geothermal waters. They have for a long been utilized in this country mainly in spas and for swimming pools. Slovakia has better geothermal conditions (23 prospective geothermal areas) than the Czech republic (3 prospective geothermal areas) and the development and utilization of geothermal energy are concentrated in Slovakia. The utilization of geothermal energy for the heating of buildings in spas commenced in 1958. Thermal energy of geothermal waters was used for direct heating through heat exchangers and in one case by a heat pump. Concentrated continuous development and utilization of geothermal energy started in 1971 (Franko et al. 1990). Practically, the first exploratory-exploitation well was situated in the central depression of the Danube basin in 1971 in the locality of Dunajská Streda (well DS-1). There the free outflow is 15.2 l/s from the well at a depth of 2,500 m. The water temperature is 92°C.

Temperature in prospective areas in Slovakia at the depth of 1000 m below the surface ranges from 30-70°C. The heat flow density values are in the range 50-110 mW/m^2 (Hurting et al., 1992). The geothermal activity is most intensive in the northern parts of the Pannonian basin, i.e. the Danube, S-Slovakian and the E-Slovakian basins. Neogene volcanics are associated with the basins. Thermal waters occur in the Inner West Carpathians. They are mostly associated with Triasic dolomites and limestones of nappes and envelope units. The aquifers have a fissure- and fissure-karst permeability. They occur in the intramontane depressions, in northern bays of the Danube basin and in the Hungarian Mid-Mountains in the basement of Tertiary sediments. Geothermal waters are also associated with Miocene-Pliocene sands and sandstones of the Danube and the S-Slovakian basins. They are less frequent in basal Paleogene and Neogene clastics and Neogene andesites and their volcanoclastics.

4.1.1 Locality

The central depression of Danube basin is located in the southern part of Slovakia, on the border of Hungary, about 20 km east of the city of Bratislava (Figure 14). This field extends in the area between Bratislava-Galanta-Nové Zámky and Komárno occupying about 4,070 km^2 (100 x 50 km) and forms the largest reservoir of geothermal water in Slovakia. Water with surface temperature of 40-90°C is at the depth of 1,000-2,500 m. On the basis of the drilling data the area was evaluated with respect to the geothermal water exploitation.

4.1.2 Hydrogeothermal characteristics

The central depression of the Danube basin has a dish-like brachysynclinal structure without respect to the pre-Pannonian basement. The reservoir is filled with Quaternary, Rumanian, Dacian, Pontian and Pannonian sediments. The Quaternary and Rumanian sediments are represented by gravels and sands, other stages by alternating clays and sandy clays with sands and sandstones. The depression originated in the Pannonian and developed up to the end of the Pliocene. It was a subsidence by bending, partly compensated by subsidence along faults.

The geothermal water reservoir is bordered from the top by a plane at a depth of 1,000 m, and from the bottom by a relatively impermeable basement sloping from all sides to its center. From the margins the basement is dipping at 30° and the dipping is decreasing towards the center. The

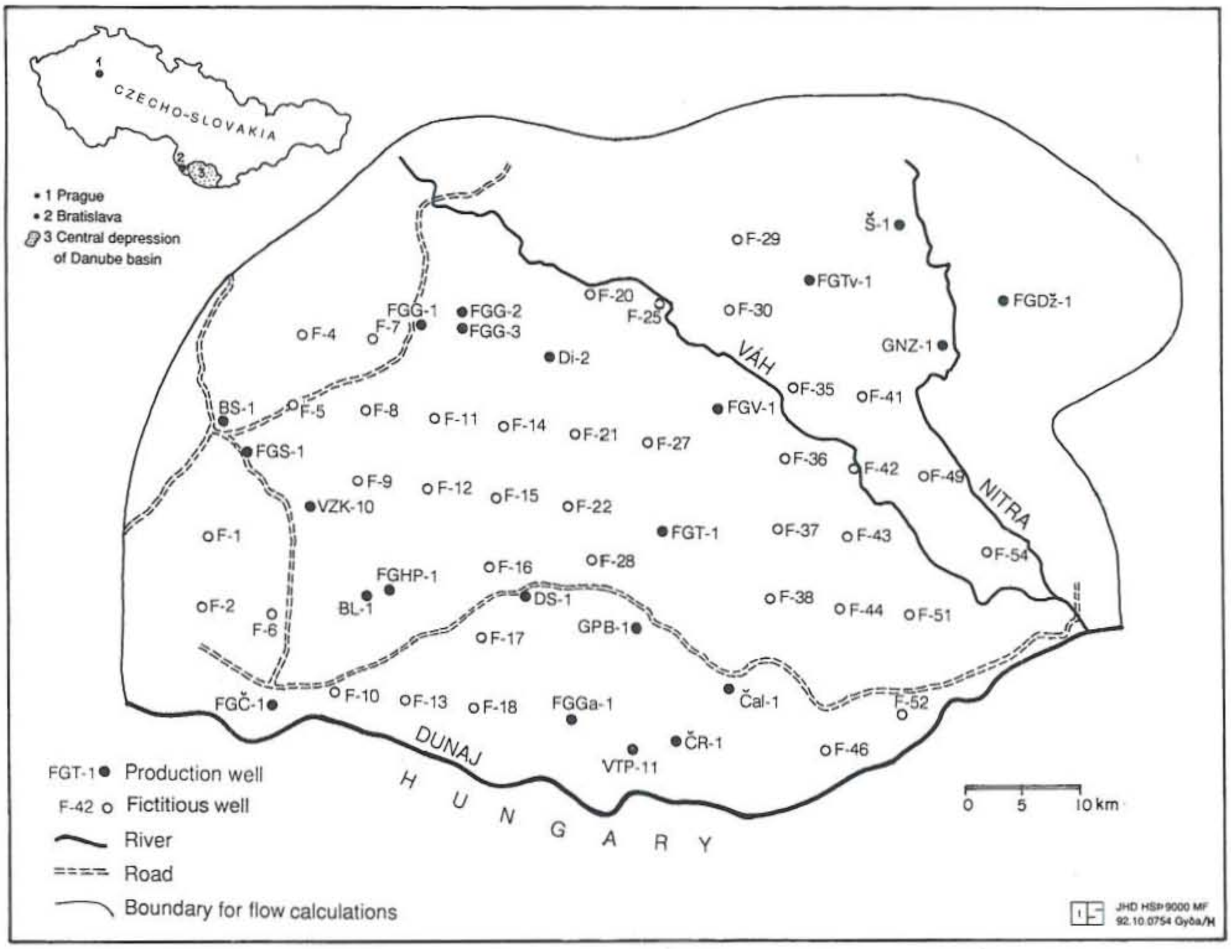

FIGURE 14: General location of the central depression of the Danube basin

maximum depth of the reservoir is 3400 m in the area of Gabčikovo i.e. in its center. The maximum length of the reservoir at the depth of 1,000 m is 60 km in the NE-SW direction and almost 70 km in the NW-SE direction. The reservoir volume takes up 4031 km^3, the collectors are 1,371 km^3 (34%).

So far 37 wells (12 investigatory, 25 exploratory-exploitation wells), 500-2,800 m deep have been drilled in the depression. Their discharge (free outflow) is 3-25 l/s and water temperatures range from 24-92°C. One well did not discharge (Franko et al. 1990a).

The geothermal gradient in the central depression varies within the limits of 35.7-43.8 °C/km, its average value is 39.4 °C/km in the depth interval of 0-2,500 m (Franko et al. 1992). At the depth of 1,000 m, the average temperature is 49°C, at 2,000 m it is 89°C and at 3,000 m it is 126°C (Table 3).

The heat flow density ranges from 70.2-92.4 mW/m^2 with an average value of 80.1 mW/m^2 (Franko et al. 1992). The geothermal waters belong to four chemical types. Two types (Na-HCO_3 with mineralization up to 1 g/l and Na-HCO_3 with mineralization of 1-5 g/l) belong genetically to petrogenic waters and two types (Na-HCO_3 or Na-Cl with mineralization of 5-10 g/l and Na-Cl with mineralization more than 10 g/l) to marinogenic waters. With depth mineralization increases, Na-HCO_3 component decreases and Na-Cl increases.

TABLE 3: Average temperatures in the central depression of the Danube basin

Depth [m]	T_{min} [°C]	T_{max} [°C]	T_{med} [°C]	Depth [m]	T_{min} [°C]	T_{max} [°C]	T_{med} [°C]
200	15	19	18	1600	64	82	73
400	22	28	25	1800	72	90	81
600	30	37	33	2000	80	98	89
800	36	45	41	2200	87	106	96
1000	43	54	49	2400	95	115	105
1200	50	63	57	3000	111	135	126
1400	56	72	65	4000	136	173	160

Incrustation properties are mainly in waters of Na-Cl type or waters with a higher CO_2 content (Bodiš and Franko 1990).

In respect of chemical composition of gases, they are methane waters, nitrogenous, methano-nitrogenous waters or waters with dominant methane. The highest methane content is characteristic of Na-Cl waters and ranges up to 83.67 vol. %. Its content increases in profiles of individual wells. The Ar-content range from 4.9×10^{-3} to 2.22 vol. %.

Among acid gases, CO_2 is dominant in geothermal waters. In well log profiles, it is associated with higher situated horizons or structures entirely recharged with CO_2.

The gas-water phase relations revealed a surficial separation range from 0.01-4.98 m^3/m^3. In the dissolved gas phase in water, CO_2 is dominant, in free gas CH_4 prevails.

4.2 Results from the calibration

Problems concerning the natural resources in the central depression were for the first time treated by Franko and Mucha (1975), on the basis of the well DS-1 in Dunajská Streda. The geothermal well was situated in a filtration environment which - on the basis of the recovery test - may be interpreted as an environment with induced infiltration by aquifer leakage from the overlying shallow gravel-sandy groundwater reservoir. From this time the central depression of the Danube basin was classified as a geothermal reservoir with leakage (Fendek and Franko, 1989). The discharge of the production wells with a pressure decrease of 0.147-0.511 MPa ranges between 3-25 l/s and the surface temperature of the water is from 24-92°C. The artesian productive system in this field is mainly due to the effect of thermolift, less by gaslift (Franko and Fendek, 1985). Geothermal water is utilized for the spaceheating of three buildings, 20 ha. of green houses, and about 35 swimming pools. Discharge which is utilized from production wells is shown in Table 4.

The first simple analytical model for the central depression was made by Fendek in 1984. Results from this model indicate that the prognostic amount of geothermal waters from free outflow with an average temperature of 60°C which can be exploited seasonally (185 days per year during winter) is about 1,027 l/s and 840 l/s for the yearly production (Fendek 1988).

Aquifers in the central depression of the Danube basin are represented by sands and sandstones aquicludes by clays, sandy clays and marlstones. The aquifers were tested by short-term (3 weeks of which 1 week is for the recovery test), long-term (2-3 months) hydrodynamical controlling measurements. Hydrodynamic results of aquifers were based on the method of unstable

TABLE 4: Discharge [l/s] from production wells

Well	Time [days]									
no.	183	365	548	730	913	1095	1278	1460	1643	1825
BS-1	12	5	12	5	12	5	12	5	12	5
FGS-1	13	5	13	5	13	5	13	5	13	5
VZK-10	20	0	20	0	20	0	20	0	20	0
BL-1	15	8	15	8	15	8	15	8	15	8
FGHP-1	20	5	20	5	20	5	20	5	20	5
FGČ-1	15	0	15	0	15	0	15	0	15	0
FGG-1	10	10	10	10	10	10	10	10	10	10
FGG-2	22	0	22	0	22	0	22	0	22	0
FGG-3	25	12	25	12	25	12	25	12	25	12
Di-2	12	12	12	12	12	12	12	12	12	12
FGV-1	8	0	8	0	8	0	8	0	8	0
FGTv-1	18	5	18	5	18	5	18	5	18	5
Š-1	5	5	5	5	5	5	5	5	5	5
FGDž-1	5	5	5	5	5	5	5	5	5	5
GNZ-1	3	3	3	3	3	3	3	3	3	3
DS-1	15	0	15	0	15	0	15	0	15	0
FGT-1	23	5	23	5	23	5	23	5	23	5
GPB-1	20	5	20	5	20	5	20	5	20	5
FGGa-1	10	10	10	10	10	10	10	10	10	10
VTP-11	15	8	15	8	15	8	15	8	15	8
ČR-1	10	5	10	5	10	5	10	5	10	5
Čal-1	10	6	10	6	10	6	10	6	10	6

groundwater flow and on consequent calculation of hydraulic parameters. Hydraulic parameters were calculated from the recovery test curves, using the Theis equation, modified by Jacob transformation. In the vertical sense the beds were tested separately gradually by single segments (open by jet perforation) from the bottom to the top. The aquifers were thus tested in the depth interval 2,503-904 m (except the wells FGB-1/A and FGS-1, where the Pannonian and Pontian sands were also tested in the depth interval 570-275 m). The **thickness of single tested segments** in the depth interval mentioned **was 87-592 m.** The **thickness of productive aquifers** ranges from **34-192 m.** After the test on single segments of wells **two or more segments** were joined by boring through the cement bridge for the purpose of geothermal water exploitation and **their thickness was 195-1093 m.** The joined segments were tested and hydraulic parameters were calculated. The transmissivity coefficient ranges from from 3.6×10^{-3} to 4.9×10^{-6} m^2/s and hydraulic conductivity coefficient ranges from 3.8×10^{-5} to 6.0×10^{-8} m/s (Fendek et al., 1988).

The total surface area covered by the mesh is about 4,070 km^2. The model was created with 2,016 nodes and 3,884 elements. Boundary conditions for the distributed groundwater flow model are established as no-flow boundaries according to geological structures forming the reservoir. As for the initial state, prior to production it was assumed that reservoir water head was constant, so that there was no hydraulic gradient in the area to begin with.

The **transmissivity** in the area covered by the model varies from **5.7×10^{-4} to 3.0×10^{-5} m^2/s** (Figure 15). The lowest value of transmissivity covers most of the external part of the basin and gradually increases towards the central part.

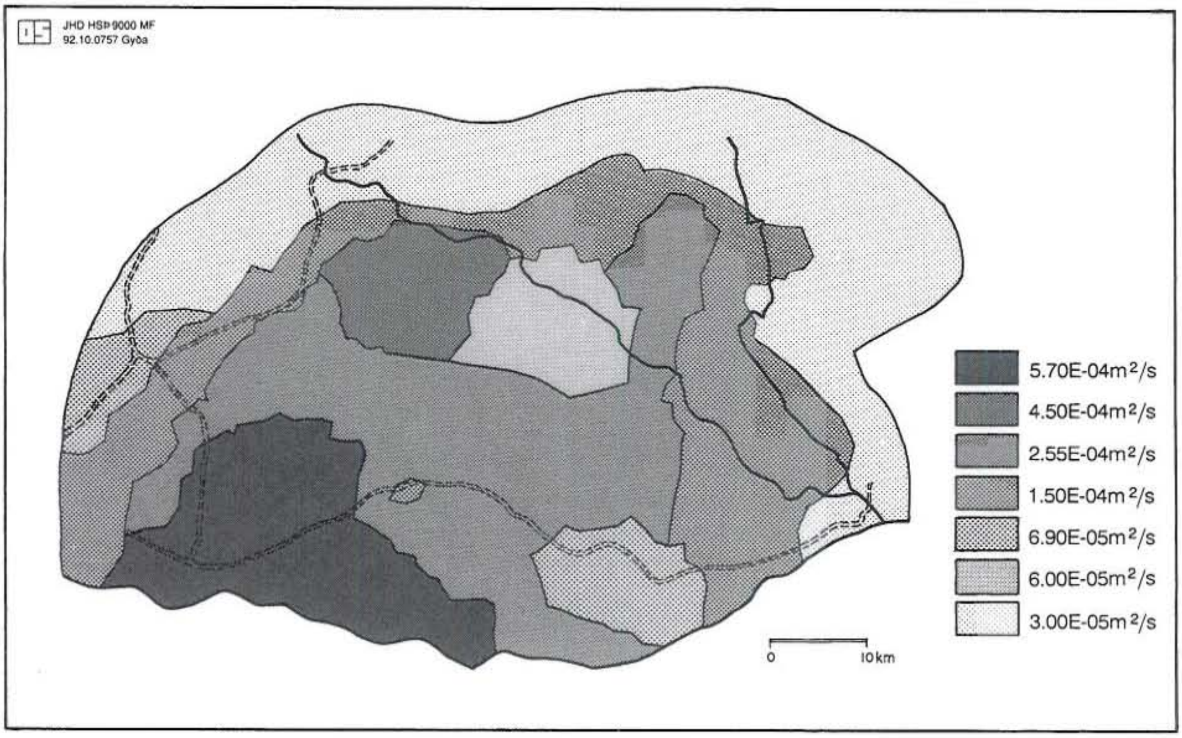

FIGURE 15: Map of transmissivity in the central depression

The area distribution of the **storage coefficient** for this model ranges from **7.5×10^{-5} to 1.1×10^{-5}**. The lower storage coefficient was used around the north and east part of the central depression. Based on some geological and geophysical information the same values were used in the vicinity of well FGV-1 Vlčany and Čal-1 Čalovo (Figure 16).

No data is available for actual anisotropy of the reservoir, hence, for the model an anisotropy angle of 0 was assumed. From well logging and some laboratory tests of cores it was found that the **porosity** of rocks ranges from **0.08-0.20**. For heat transport problem, the porosity value of **0.13** was used.

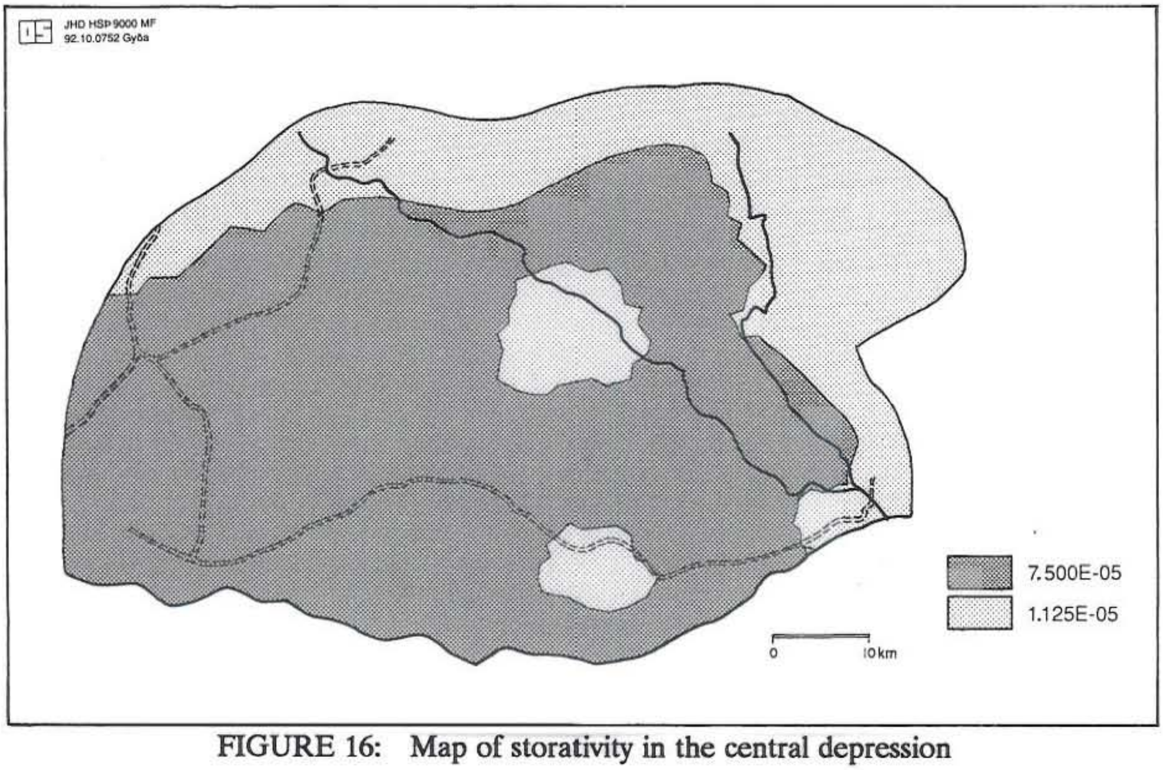

FIGURE 16: Map of storativity in the central depression

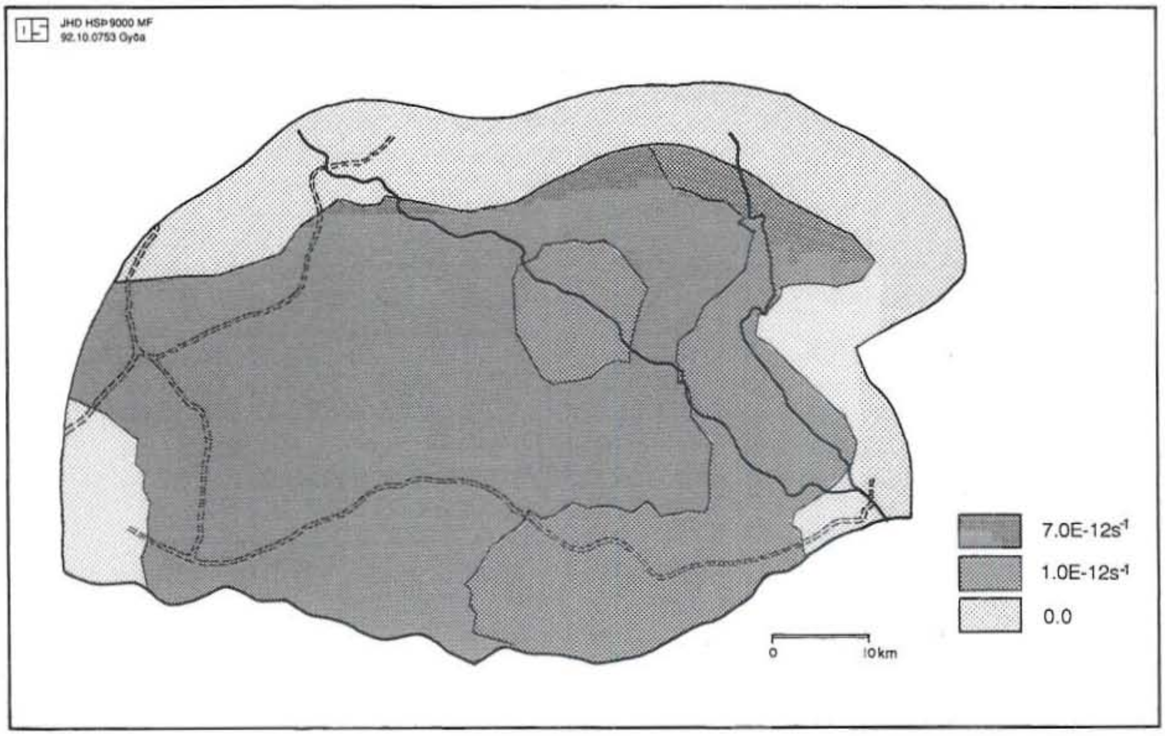

FIGURE 17: Map of leakage coefficient in the central depression

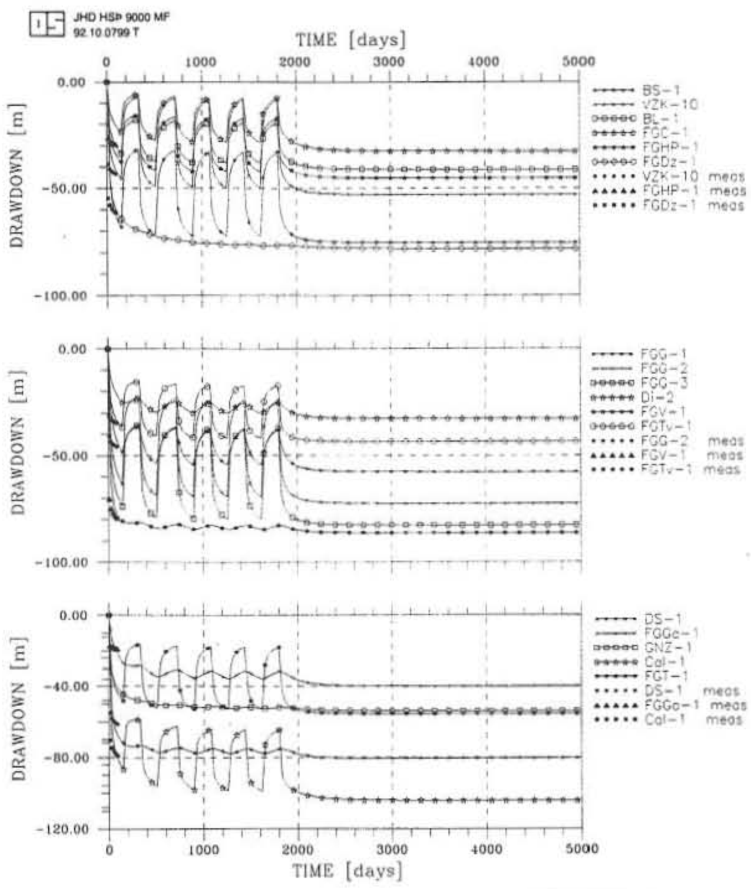

FIGURE 18: Calculated drawdown for production wells

The **leakage coefficient** ranges from **7.0×10^{-12} to 1.0×10^{-12} s^{-1}**. The highest value was used for the central part of the reservoir and 0 for the outer western, northern and eastern parts of the reservoir (Figure 17). In the five years of geothermal water production with mainly seasonal exploitation, the decline of the water level and temperature in the reservoir was not measured. Results from a distributed parameter model show that after **10 years** production of **308 l/s** (refer to Table 4) of geothermal water the reservoir has a relatively steady-state condition (Figure 18).

A map of calculated drawdown for the production wells is shown in Figure 19. From this figure, it is shown that the highest drawdown (-100 m) is around well Čal-1 Čalovo and the lowest drawdown (-50 m) is in the center and western part of the reservoir.

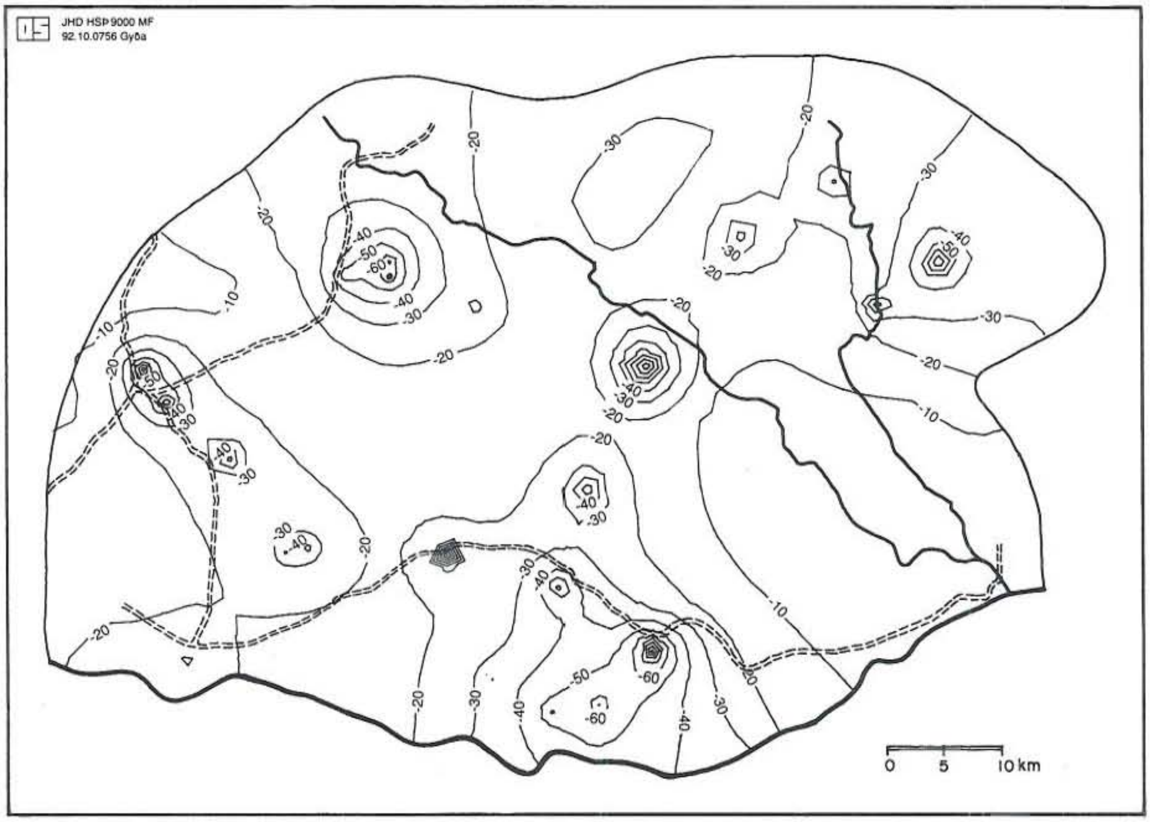

FIGURE 19: Map of calculated drawdown [m] for production wells

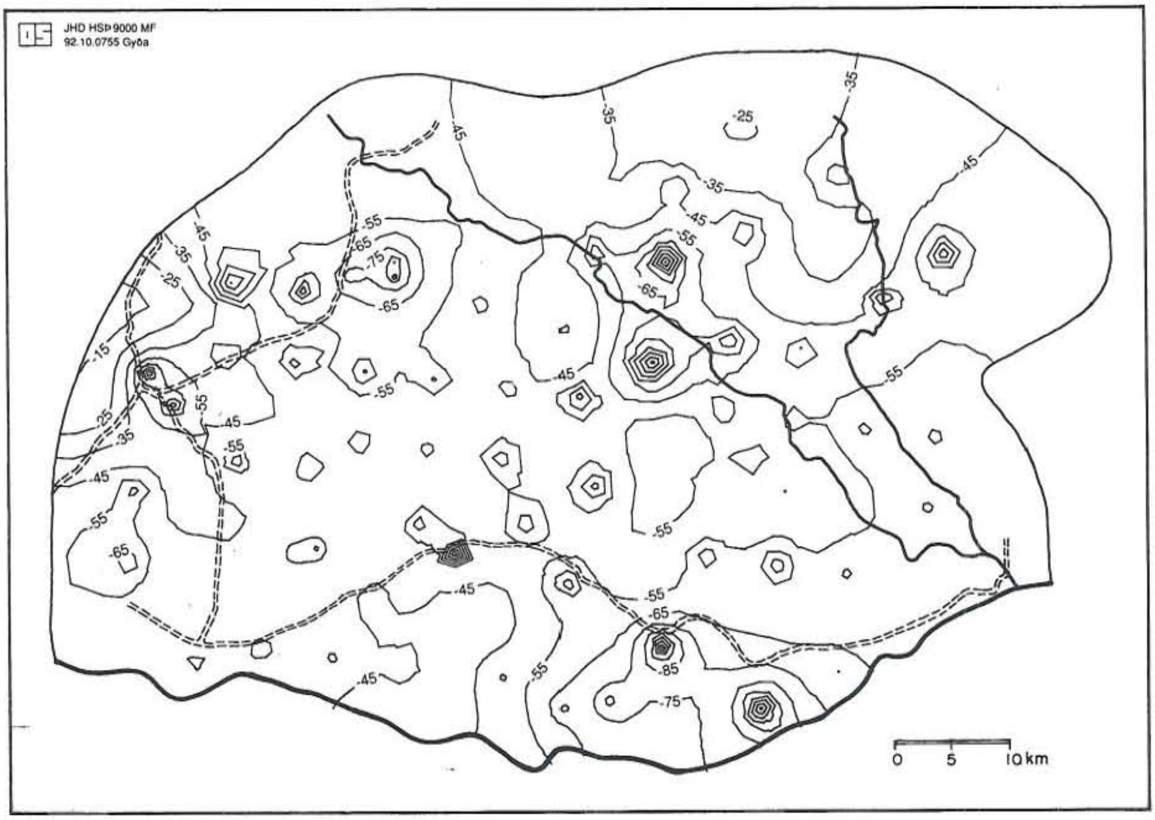

FIGURE 20: Map of calculated drawdown [m] for production and fictitious wells

For future prediction, the production from the central depression of the Danube basin is increased by about 424 l/s (Table 5) due to some fictitious wells (refer to Figure 14). A map of calculated drawdown for production and fictitious wells is shown in Figure 20. For this case the total production from the central depression of Danube basin is 732 l/s.

The heat transport calculation can be used to test the appropriate choice of leakage coefficient, aquifer thickness and porosity. The parameters used in solving the heat transport problem are as follows:

Porosity of reservoir:	*13%;*
Longitudinal dispersivity:	*80 m;*
Retardation constant:	*0.191;*
Aquifer thickness:	*250 m.*

The relative temperature of cold water used was 0.25. Since the temperature in the reservoir is not constant, it was considered to use an arbitrary number of 1 to represent the temperature at a certain part in the reservoir. Results of the calculations are shown in Figure 21. These confirm that there had been no significant changes in reservoir temperatures during the 30 years of exploitation. The highest temperature decline is around the locality of Galanta (well FGG-3), but it is only 0.0043, which represents a drop from the arbitrary number of 1 to 0.9957 (refer to Figure 21). For the temperature 60°C which is on locality Galanta at a depth 1,500 m this temperature decline is represented by 0.26°C.

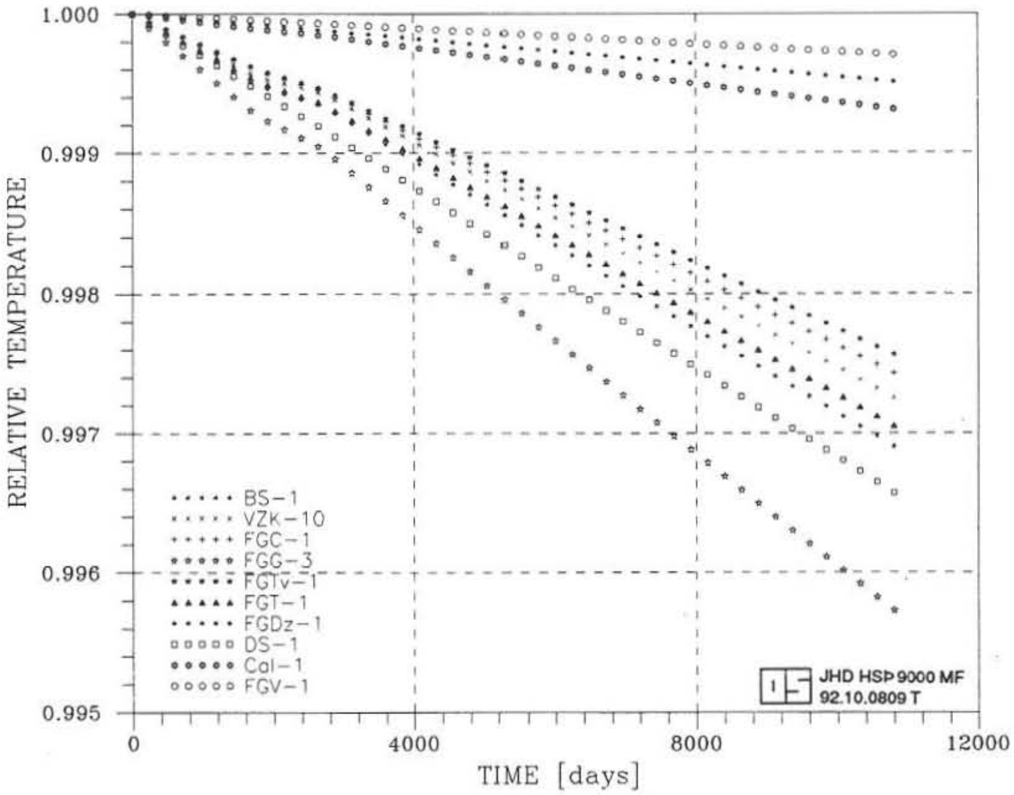

FIGURE 21: Temperature decline in production wells after fictious production

TABLE 5: Discharge from fictitious wells

Well no.	Node no.	Discharge [l/s]	Well no.	Node no.	Discharge [l/s]
F - 1	23	11	F - 22	45	17
F - 2	24	12	F - 25	50	12
F - 4	26	6	F - 27	48	15
F - 5	27	7	F - 28	155	16
F - 6	29	11	F - 29	52	9
F - 7	33	15	F - 30	53	15
F - 8	32	15	F - 35	60	15
F - 9	31	5	F - 36	59	10
F - 10	30	17	F - 37	58	9
F - 11	34	18	F - 38	57	15
F - 12	35	12	F - 41	62	8
F - 13	36	17	F - 42	63	5
F - 14	41	15	F - 43	64	6
F - 15	40	8	F - 44	65	16
F - 16	39	17	F - 46	67	10
F - 17	38	7	F - 49	71	5
F - 18	37	13	F - 51	69	4
F - 20	43	9	F - 52	68	3
F - 21	44	10	F - 54	75	4

5. RESULTS AND CONCLUSIONS

The prime objective of this work is to create models approximating the natural conditions of the Laugarnes geothermal field and the central depression of the Danube basin, using the field data for the last 30 years. Through these models, the reservoir parameters and features of the fields were described and some predictions of their future behaviour were made. All available geological , geophysical and geochemical information, along with field measurement data were collected and carefully studied to understand how all these factors contributed to the overall picture of the geothermal reservoir.

The study of the Laugarnes geothermal reservoir, applying the distributed model, presents results that are very close to the measured field data. This indicates a correct approach and that the model is reliable for similar reservoir modelling and future forecasting. However, as the methods use only linear functions in their mathematical models, the effects of turbulence and skin impact are not taken into account. This means that the drawdown values in close proximity to the pumping wells cannot always be considered accurate.

The measurements from the field indicate higher values of SiO_2 in 1962. Over the production period of 30 years, the effects of water discharge are observed very clearly with a lowering of the water level and decline of the SiO_2 content.

For the calibration of the model, the measured data from 16 wells was used. The good fit with the model for drawdown, using the equation for delayed yield, shows that the reservoir is controlled by two different storage mechanisms. At the start of production, storage is controlled by liquid/formation compressibility with characteristic values for the confined aquifers ranging from 1.6×10^{-3} to 1.6×10^{-4}. In later production, the storage coefficient is controlled by the mobility of the free surface with a value of approximately 0.011, which is near to the effective porosity.

From the trend of the measured and calculated curves for the drawdown obtained from distributed groundwater flow model, it is quite obvious that with present production no steady-state conditions in the reservoir can be reached until year 2012. So, the recharge in the system is much less than the production for the present drawdown.

Results from the distributed parameter model for the central depression of the Danube basin shows that during the production period of 30 years, the reservoir has reached a relatively steady-state condition for a discharge of about 308 l/s. When production from this reservoir is increased by about 424 l/s, then the drawdown is expectedly increased to about 20-50 m in the different parts of the central depression. But this theoretical reservoir model must be checked against real measurements which are not currently available for the past several years in the central depression of the Danube basin.

ACKNOWLEDGEMENTS

The author is grateful to Dr. Snorri Pall Kjaran for his help and guidance during the formation of this report. Thanks are also expressed to Sigurdur Larus Holm for his patient and detailed assistance in acquainting me with the AQUA program.

I would like to thank Dr. Ingvar Birgir Fridleifsson, the director of the UNU Geothermal Training Programme for giving me the chance to attend the UNU geothermal course and for providing excellent work conditions during my entire study.

I also wish to extend my gratitude to the government of Iceland for this Fellowship. My thanks also goes to Ludvik S. Georgsson, Marcia Vilhjalmsdottir for carefully editing the report and to all the ladies in the drawing room for completing some of the figures in this report.

I am very grateful to all the lecturers for their comprehensive presentations, particularly to all the staff of the Reservoir Engineering Unit for their willingness to share their knowledge and experience.

Finally, the author is grateful to Dr. Tomáš Koráb, the director of the Dionýz Štúr Institute of Geology in Bratislava for giving the opportunity to participate in the training programme.

NOMENCLATURE

a_L	-longitudinal dispersivity	[m]
a_T	-transversal dispersivity	[m]
b	-aquifer thickness	[m]
c	-solute concentration	[kg/m^3]
c_o	-solute concentration of vertical inflow	[kg/m^3]
c_w	-solute concentration of injected water	[kg/m^3]
C_l	-specific heat capacity of the liquid	[kJ/kg°C]
C_s	-specific heat capacity of the porous media	[kJ/kg°C]
D_m	-molecular diffusivity	[m^2/s]
D_h	-heat diffusivity	[m^3/s]
D_{xx}	-dispersion coefficient in x direction	
D_{yy}	-dispersion coefficient in y direction	
h	-groundwater head	[m]
h_o	-head in upper aquifer	[m]
k	-permeability of the semi-permeable layer	[m/s]
K_d	-distribution coefficient	
m	-aquitard thickness	[m]
R	-infiltration	[mm/year]
R_d	-retardation coefficient	
S	-storage coefficient	
t	-time	[s]
T	-temperature	[°C]
T_o	-temperature in vertical inflow	[°C]
T_{xx}	-transmissivity in x direction	[m^2/s]
T_{yy}	-transmissivity in y direction	[m^2/s]
Q	-pumping/injection rate	[m^3/s]
v	-velocity	[m/s]
v_x	-velocity in x direction	[m/s]
v_y	-velocity in y direction	[m/s]

Greek symbols:

β_c	-retardation constant (mass transport)	
β_h	-retardation constant (heat transport)	
γ	-leakage	[m/s]
κ	-time constant	[s]
λ	-decay constant	[s^{-1}]
ϱ_l	-density of the liquid	[kg/m^3]
ϱ_s	-density of the porous media	[kg/m^3]
ϕ	-porosity	

REFERENCES

Arnason, B., and Tomasson, J., 1970: Deuterium and chloride in geothermal studies in Iceland. Geothermics, Special issue, V.2, 1405-1415.

Arnason, B., 1977: Groundwater systems in Iceland traced by deuterium. Soc. Sci. Islandica, Publ. 42, 236 pp.

Bodiš, D., and Franko, O., 1990: Chemical composition of geothermal waters in central depression of Danube basin. Geothermal Res. Counc., Trans., Vol. 14, Part II, 853-855.

Bodvarsson, G.S., Pruess, K., and Lippman, M.J., 1986: Modelling of geothermal systems. J. Pet. Tech. (Sept. 1986), 1007-1021.

Bodvarsson, G.S., and Witherspoon, P.A., 1989: Geothermal reservoir engineering. Part I. Geothermal Science and Technology, 2-1, 1-68.

Fendek, M., 1988: Hodnotenie tepelno-energetického potenciálu geotermálnych vôd centrálnej depresie podunajskej panvy. Geologický průzkum, roč. 30, č. 11, SNTL Praha, (in Slovak), 327-329.

Fendek, M., Franko, O., and Remšik, A., 1988: Členenie nádrže geotermálnych vôd a hodnotenie hydrogeologických údajov v centrálnej depresii podunajskej panvy z hľadiska ich výskytu. Zbornik prispevkov 9. celoštátnej hydrogeologickej konferencie v Pardubiciach (in Slovak).

Fendek, M., and Franko, O., 1989: Evaluation of geothermal water resources in central depression of Danube basin. XIV. Congress CBGA, Sofia, 1096-1099.

Franko, O., and Mucha, I., 1975: Geothermal resources of the central depression of the Danubian basin in Slovakia. Second U.N. Symposium on the Development and Use of Geothermal Resources, San Francisco, Proceedings, 979-992.

Franko, O. and Fendek, M., 1985: K principu termosifónu termálnych vôd v Západných Karpatoch. Geologické Práce, Správy 82, Geol. Úst. D. Štúra, Bratislava (in Slovak), 135-155.

Franko, O., Bodiš, D., Fendek, M., and Remšik, A., 1990: Outline of geothermal activity in Czecho-Slovakia. Geothermal Res. Counc., Trans., Vol. 14, Part I, 31-40.

Franko, O., Fendek, M., Remšik, A., and Král, M., 1990a: Geothermal energy in central depression of Danube (Pannonian) basin. Geothermal Res. Counc., Trans., Vol. 14, Part II, 879-887.

Franko, O., Bodiš, D., Fendek, M., Franko, J., Král, M., Remšik, A., and Vranovská, A., 1992: Geothermal fields of Slovakia. International conference on industrial uses of geothermal energy. Reykjavik, Iceland, 14 pp.

Fridleifsson, I.B., 1973: Petrology and structure of Esja quaternary volcanic region, SW-Iceland. Unpublished Ph.D. Thesis. Oxford University.

Grant, M.A., Donaldson, I.G., and Bixley, P.F., 1982: Geothermal reservoir engineering. Academic press, New York, 369 pp.

Hettling, H., K., 1984: The chemical and isotopic changes in the low temperature areas of Laugarnes, Ellidaar and Reykir. UNU G. T. P., Iceland, report 3, 52 pp.

Hurting, E., Čermák, V., Haenel, R., and Zui, V., 1992: Geothermal atlas of Europe - explanatory text. Geoforschung Zentrum, Postdam, 21-25.

Palmason, G., 1967: On heat flow in Iceland in relation to the Mid-Atlantic Ridge. Societas Scientarium Islandica, V. 38, 111-127.

Thorsteinsson, T., and Eliasson, J., 1970: Geohydrology of the Laugarnes hydrothermal system in Reykjavik, Iceland. Geothermics, special issue, V.2, 1191-1204.

Tomasson, J., Fridleifsson, I.B. and Stefansson, V., 1975: A hydrological model for the flow of thermal water in southwestern Iceland with special reference to the Reykir and Reykjavik thermal areas. Second U.N. Symposium on the Development and Use of Geothermal Resources, San Francisco, Proceedings, 643-648.

Vatnaskil Consulting Engineers, 1991: AQUA user's manual. Vatnaskil, Reykjavik.